Freie Universität Berlin

Fabrication and Modification of Carbon Electrode Materials for Vanadium Redox Flow Batteries

Inaugural-Dissertation

to obtain the academic degree

Doctor rerum naturalium (Dr. rer. nat.)

submitted to the Department of Biology, Chemistry and Pharmacy

of Freie Universität Berlin

by

Abdulmonem Fetyan

Berlin, 2018

I hereby declare that the thesis submitted is my own unaided work. All direct or indirect sources used are acknowledged as references.

Abdulmonem Fetyan Berlin, 01.11.2018

Supervisor: Prof. Dr. Christina Roth

Second examiner: Prof. Dr. Nora Kulak

Date of the defense: 19.12.2018

Abstract

Vanadium redox flow batteries (VRFBs) are amongst the most promising energy storage systems for storing renewable energies on a large scale. However, the system still has some challenges which limit its widespread application in industry. For instance, the unsatisfactory activity together with insufficient long-term stability of the state-of-the-art commercial activated carbon electrode (i.e., carbon felts) are the most known issues referenced in literature. This thesis introduces two novel solutions for the aforementioned problems: (i) fabrication of non-woven carbon nanofiber networks as alternative, efficient and stable electrodes and (ii) improving the performance of the commercial carbon felt electrodes via coating their surfaces with metal oxide nanostructures. Additionally, the hydrogen evolution reaction, a parasitic side reaction, which is believed to have detrimental impact on the performance of VRFBs, will be investigated at different operating temperatures.

Non-woven polyacrylonitrile-based carbon nanofiber networks with a very high electrochemically active surface area were first produced by the scalable electrospinning approach and then directly used as an electrode in a vanadium redox flow battery. Using five sheets of polyacrylonitrile-based electrospun nanofibers achieved ~10% increase in the energy efficiency compared to the commercial carbon felt at current densities of 15 $mAcm^{-2}$. Furthermore, low-cost highly active carbon-carbon composite freestanding nanofibers were produced by electrospinning a mixture of polyacrylonitrile and carbon black powder using poly acrylic acid (PAA) as binder. PAA enables the loading with higher amounts of the relatively cheap carbon black material. This results in an increase of the productivity of the electrospun carbon nanofibers at lower cost together with simultaneously enhancing the performance of the battery. Battery test results demonstrated a promising performance for the newly designed electrospun carbon fibers as negative and positive electrodes of vanadium redox flow batteries at current densities below 60 $mAcm^{-2}$.

The damaging role of the parasitic hydrogen evolution reaction (HER) in the negative half-cell of the vanadium redox flow battery on the performance of the commercial carbon felt electrodes was studied at different temperatures. Increasing the temperature resulted in a better catalytic performance for both the positive and negative half-cell reactions. Nevertheless, higher temperature significantly enhanced also the undesired HER at the negative side. This led to a decrease in the coulombic efficiency attributed to the higher amount of generated hydrogen causing faster fading of the overall VRFBs performance. Due

to rapid degradation of the commercial carbon felts resulting from the corrosion of their fibers. To minimize the degradation of the commercial carbon felt electrodes and therefore extend the lifetime of the battery, neodymium oxide (Nd_2O_3) nanoparticles were chemically deposited onto the fibers of the carbon felt by a precipitation method in non-aqueous solution. Nd_2O_3 modified carbon felts showed 4 times higher stability compared to the unmodified thermally activated carbon felt after 50 consecutive charge/discharge cycles. Moreover, Nd_2O_3 modified felts retained their original performance after exchanging the electrolyte, indicating less degradation occurred. Additionally, they could maintain their oxygen donating functionalities compared to the thermally activated commercial carbon felt.

Zusammenfassung

Vanadium-Redox-Flow-Batterien (VRFBs) gehören zu den vielversprechenden Systemen für die Speicherung erneuerbarer Energien in großem Umfang. Das System hat allerdings noch einige Herausforderungen zu überwinden, die seine bisherige breite Anwendung in der Industrie einschränken. Zu den bekanntesten Problemen gehören die nicht zufriedenstellende Aktivität sowie eine unzureichende Langzeit beständigkeit der kommerziellen aktivierten Kohlenstoffelektroden (d.h. Kohlenstofffilze), auf die in der Literatur Bezug genommen wird. Diese Dissertation stellt zwei neuartige Lösungen für die oben genannten Probleme vor: (i) Herstellung von Kohlenstoffnanofasernetzwerken als alternative, effiziente und stabile Elektroden und (ii) Verbesserung der Leistung der kommerziellen Kohlenstofffilzelektroden durch Beschichten ihrer Oberflächen mit Metalloxidnanostrukturen. Zusätzlich wird die Wasserstoffentwicklungsreaktion, eine parasitäre Nebenreaktion, von der angenommen wird, dass sie sich negativ auf die Leistung von VRFBs auswirkt, bei verschiedenen Betriebstemperaturen untersucht.

Polyacrylnitrilbasierte Kohlenstoffvliese, die eine sehr hohe elektrochemisch aktive Oberfläche besitzen, wurden zunächst mit dem skalierbaren Elektrospinnverfahren hergestellt und fanden anschließend als Elektrode in einer Vanadium-Redox-Flow-Batterie Anwendung. Durch die Verwendung von fünf dünen Schichten der polyacrylnitrilbasierten Elektrospinn-Nanofasern wurde eine um ca. 10% höhere Energieeffizienz erreicht als bei einem handelsüblichen Kohlenstofffilz bei Stromdichten von 15 $mAcm^{-2}$. Darüber hinaus wurden kostengünstige hochaktive Kohlenstoff-Kohlenstoff-Komposite durch Elektrospinnen einer Mischung aus Polyacrylnitril und Rußpulver unter Verwendung von Polyacrylsäure (PAA) als Bindemittel hergestellt. PAA ermöglicht eine höhere Beladung des relativ preisgünstigen Rußmaterials. Dies führt zu einer Erhöhung der Produktivität der neuartigen gesponnenen Kohlenstoffnanofasern bei entsprechend geringeren Kosten und gleichzeitiger Verbesserung der Leistung der Batterie. Batterietestergebnisse zeigten eine vielversprechende Leistung für die entwickelten elektrogesponnenen Kohlenstofffasern als negative und positive Elektrode in Vanadium Redox-Flow-Batterien bei Stromdichten unter 60 $mAcm^{-2}$.

Der negative Effekt der parasitären Wasserstoffentwicklungsreaktion (HER) auf die Leistung der handelsüblichen Kohlenstofffilz-Elektroden in der negativen Halbzelle der VRFB wurde bei verschiedenen Temperaturen untersucht. Die Erhöhung der Temperatur führte zu einer besseren katalytischen Leistung sowohl für die positive als auch für die negative

Halbzellenreaktion. Trotzdem verstärkte eine höhere Temperatur auch die unerwünschte HER auf der negativen Seite. Dies führte zu einer Abnahme der Coulomb-Effizienz, die auf die höhere Menge an erzeugtem Wasserstoff zurückzuführen ist, was wiederum zu einem schnelleren Einbruch der Gesamtleistung der VRFB führt. Hervorgerufen wird dies durch die schnelle Zersetzung der handelsüblichen Kohlenstofffilze infolge der Korrosion ihrer einzelnen Fasern. Um die Degradation der handelsüblichen Kohlenstofffilzelektroden zu minimieren und folglich die Lebensdauer der Batterie zu verlängern, wurden Neodymoxid (Nd_2O_3) -Nanopartikel durch ein Ausfällungsverfahren in einer nicht wässrigen Lösung chemisch auf den Fasern des Kohlefilzes abgeschieden. Mit Nd_2O_3 modifizierte Kohlenstofffilze zeigten nach 50 aufeinanderfolgenden Lade- und Entladezyklen eine viermal höhere Stabilität im Vergleich zu nicht modifizierten, thermisch aktivierten Kohlefilzen. Darüber hinaus behielten Nd_2O_3-modifizierte Filze nach dem Austauschen des Elektrolyts ihre ursprüngliche Leistungsfähigkeit bei, was darauf hinweist, dass ein geringerer Abbau stattgefunden hat. Ebenso verblieben hier die funktionellen Sauerstoffgruppen im Vergleich zu den thermisch aktivierten kommerziellen Kohlefilzen auf der Vliesoberfläche.

List of Publications

Peer reviewed articles included in this thesis

1. Fetyan, A.; Derr, I.; Kayarkatte, M. K.; Langner, J.; Bernsmeier, D.; Kraehnert, R.; Roth, C., Electrospun Carbon Nanofibers as Alternative Electrode Materials for Vanadium Redox Flow Batteries. *ChemElectroChem* **2015,** *2* (12), 2055-2060, DOI: 10.1002/celc.201500284.

2. Fetyan, A.; Schneider, J.; Schnucklake, M.; El-Nagar, G. A.; Banerjee, R.; Bevilacqua, N.; Zeis, R.; Roth, C., Comparison of Electrospun Carbon−Carbon Composite and Commercial Felt for Their Activity and Electrolyte Utilization in Vanadium Redox Flow Batteries. *ChemElectroChem* **2018** (accepted), DOI: 10.1002/celc.201801128.

3. Fetyan, A.; El-Nagar, G. A.; Derr, I.; Kubella, P.; Dau, H.; Roth, C., A neodymium oxide nanoparticle-doped carbon felt as promising electrode for vanadium redox flow batteries. *Electrochimica Acta* **2018,** *268*, 59-65, DOI: 10.1016/j.electacta.2018.02.104.

4. Fetyan, A.; El-Nagar, G. A.; Lauermann, I.; Schnucklake, M.; Schneider, J.; Roth, C., Detrimental role of hydrogen evolution and its temperature-dependent impact on the performance of vanadium redox flow batteries. *Journal of Energy Chemistry* **2018** (accepted), DOI: 10.1016/j.jechem.2018.06.010.

Peer reviewed articles not included in this thesis

5. Derr, I.; Fetyan, A.; Schutjajew, K.; Roth, C., Electrochemical analysis of the performance loss in all vanadium redox flow batteries using different cut-off voltages. *Electrochimica Acta* **2017,** *224*, 9-16.

6. Schnucklake, M.; Kuecken, S.; Fetyan, A.; Schmidt, J.; Thomas, A.; Roth, C., Salt-templated porous carbon–carbon composite electrodes for application in vanadium redox flow batteries. *Journal of Materials Chemistry A* **2017,** *5* (48), 25193-25199.

7. Derr, I.; Przyrembel, D.; Schweer, J.; Fetyan, A.; Langner, J.; Melke, J.; Weinelt, M.; Roth, C., Electroless chemical aging of carbon felt electrodes for the all-vanadium redox flow battery (VRFB) investigated by Electrochemical Impedance and X-ray Photoelectron Spectroscopy. *Electrochimica Acta* **2017,** *246*, 783-793.

8. El-Nagar, G. A.; Derr, I.; Fetyan, A.; Roth, C., One-pot synthesis of a high performance chitosan-nickel oxyhydroxide nanocomposite for glucose fuel cell and electro-sensing applications. *Applied Catalysis B: Environmental* **2017,** *204*, 185-199.

9. El-Nagar, G. A.; Hassan, M. A.; Fetyan, A.; Kayarkatte, M. K.; Lauermann, I.; Roth, C., A promising N-doped carbon-metal oxide hybrid electrocatalyst derived from crustacean's shells: Oxygen reduction and oxygen evolution. *Applied Catalysis B: Environmental* **2017,** *214*, 137-147.

10. Derr, I.; Bruns, M.; Langner, J.; Fetyan, A.; Melke, J.; Roth, C., Degradation of all-vanadium redox flow batteries (VRFB) investigated by electrochemical impedance and X-ray photoelectron spectroscopy: Part 2 electrochemical degradation. *Journal of Power Sources* **2016,** *325*, 351-359.

Table of Contents

Abbreviations and Acronyms

BET	Brunauer–Emmett–Teller theory
CE	Current efficiency
CF	Carbon Felt
CV	Cyclic voltammetry
DLC	Double layer capacitance
ECSA	Electrochemically active surface area
EDX	Energy dispersive X-ray spectroscopy
EE	Energy efficiency
EIS	Electrochemical impedance spectroscopy
GC	Glassy carbon
HER	Hydrogen evolution reaction
OCP	Open circuit potential
PAA	Poly acrylic acid
PAN	Polyacrylonitrile
R_{ct}	Charge transfer resistance
RFB	Redox flow battery
R_u	Contact resistance
SEM	Scanning electron microscopy
SCE	Saturated calomel electrode
SHE	Standard hydrogen electrode
SOC	State of charge
TXRF	Total X-ray fluorescence
VE	Voltage efficiency
VRFB	Vanadium redox flow battery
XCT	X-ray computed tomography
XPS	X-ray photoelectron spectroscopy
XRD	X-ray diffraction

1. Introduction

The utilization of renewable energy sources, such as solar and wind, has enormously increased in recent years. However, the employment of these sources is limited due to their characteristics of being intermittent and often unpredictable, and, as such, renewable energy currently share a small percentage of the global primary power sources. Recent analysis proposed that if non-dispatchable renewable energy surpasses 20% of the energy-generation capacity without storing excess energy, the electric grid could become destabilized.[1] To increase the proportion of energy generated by renewables, as announced by the German government, up to 55% by 2035 and 80 % by 2050,[2] reliable storage systems are needed. There are several different storage devices available depending on applications. For instance, supercapacitors or fly wheels are appropriate devices for high output energy and very fast response time, compressed air energy storage or pump storage or batteries for medium capacity range, and secondary energy carriers such as hydrogen or methane for the longer storage range.[1, 3-6] Cost of the systems and response time are the main factors affecting the implementation of the storage devices on large scale. Most used and popular battery technologies are the lead-acid batteries and Li-ion batteries. Compared to Li-ion batteries, lead-acid batteries are considered as low cost storage systems but also have a limited life-time for charging/discharging cycles and therefore should be substituted regularly. While Li-ion batteries have higher energy densities and better profile of charging/discharging, they necessitate higher costs. Redox flow batteries (RFB) can be considered reliable and long-lasting storage devices when taking into account the long life-time and low maintenance cost of these storage systems, besides other characteristics, such as large capacities, negligible self-discharge and independently scaled energy and power density.[7] Unlike conventional batteries, the long life-time rated at 10,000 cycles in RFBs is associated with the lack of phase change (expansion and contraction) at the electrodes during cycling which would result in their degradation over time. Several studies have been published in the last two decades to increase the performance of carbon electrodes by activating and modifying the materials.[8-15] Most of these studies focused on the increase of surface functional groups to enhance the electrode kinetics. However, recent literature[16-18] reported degradation phenomena and poor long-term stability of the activated felts in RFBs highlighting the need to investigate the root of the problem and to find new routes to explore more active and stable carbon felts to be used as alternative reliable electrode materials.

1.1. Redox flow batteries

Since 1971 the concept of redox flow cells and many developments associated with this technology were under investigation mainly in Japan. The use of different redox states of various soluble species and inert electrodes eliminates undesirable electrode structural changes in the system. Unlike secondary battery systems, the energy in RFBs is stored chemically in the electrolytes in two half-cells and the energy storage capacity is determined by the concentration of the redox species and the volume of the used electrolyte, while the power of the system can be tuned depending on the current densities and number of cells in the stack.[19] Therefore, RFBs provide independent storage capacity and power output, which makes RFBs pioneer systems which satisfy the required power and energy demand for different applications.[20] Many organic and inorganic redox species have been studied for the application as electroactive couples in RFB.[21-22] All-vanadium RFBs (VRFBs) is the most promising and studied RFB to date.[5, 21] The system was proposed by Skyllas-Kazacos and coworkers in 1984 at the University of New South Wales, Australia where the use of one element (vanadium) in both half-cells as electroactive species could solve the poisoning associated with cross contamination of different redox ions across the membrane. A typical VRFB system is shown in Figure 1. The system consists of two external reservoirs for storing the electrolytes, an electrochemical cell for converting the energy, and pumps for circulating the electrolytes between the electrochemical cell and the reservoirs.

In a VRFB, the four oxidation states of vanadium are being utilized in the two half-cell reactions. The electroactive species are the V(II)/V(III) redox couple in the negative side and V(IV)/V(V) in the positive side.

The electrochemical half-cell reactions are given as follows:

Positive electrode reaction:

$$VO^{2+} + H_2O \underset{\text{charge}}{\rightleftharpoons} VO_2^{+} + 2H^{+} + e^{-} \qquad E_o = 1.0\ V \text{ vs. } SHE \qquad (1)$$

Negative electrode reaction:

$$V^{3+} + e^{-} \underset{\text{charge}}{\rightleftharpoons} V^{2+} \qquad E_o = -0.26\ V \text{ vs. } SHE \qquad (2)$$

And the overall cell potential at room temperature is 1.26 V.

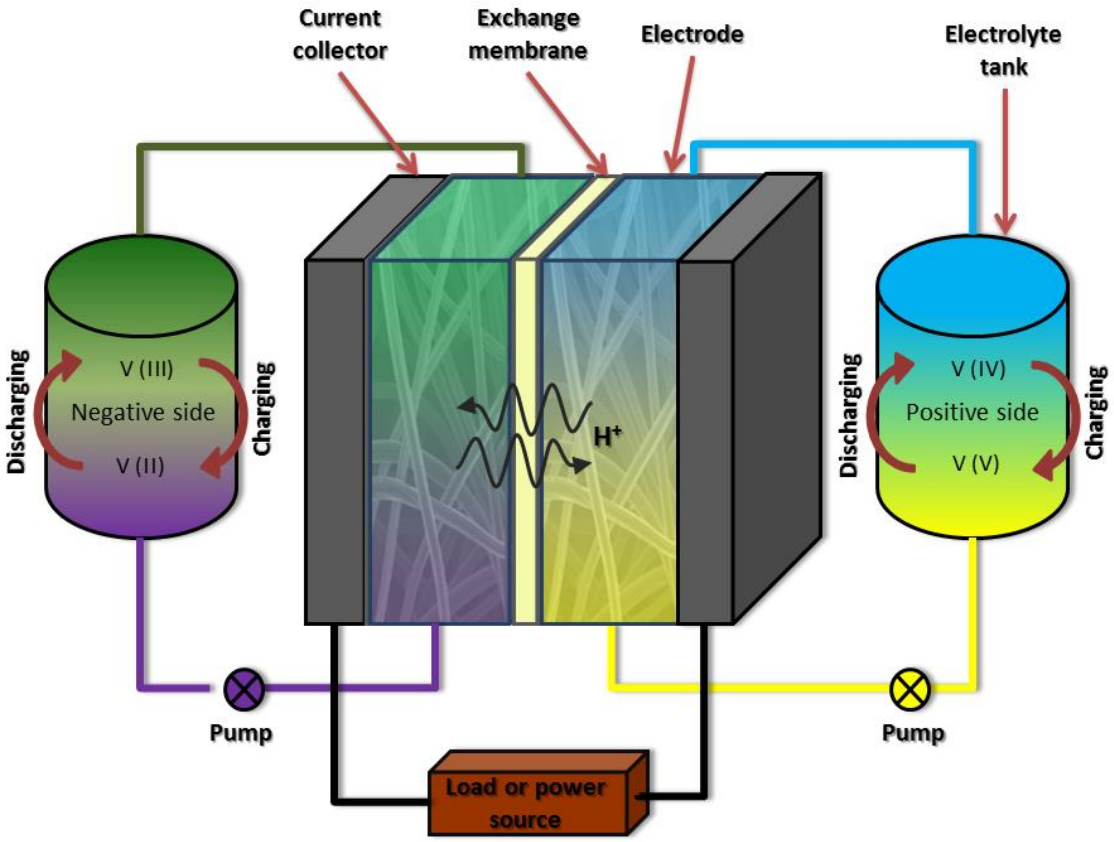

Figure 1: Schematic representation of vanadium redox flow battery working principle.

The used electrolyte is usually consisting of 1.5-2 M vanadium solution in 2 M H_2SO_4, and provides a maximum theoretical energy density of 19-38 WhL^{-1}. The increased concentration of vanadium is necessary to achieve highest volumetric and gravimetric energy densities.[7] However, at this limit, the precipitation of V(V) is possible at elevated temperatures above 40 °C.[23-24] To prevent such precipitation, various additives, such as potassium sulfate, sodium hexametaphosphate, hydrochloric acid or phosphoric acid,[25-26] are usually added to the electrolyte to stabilize the solution. For instance, Li et al. succeeded in increasing the vanadium concentration to be ~2.5 M via mixing sulfate and chloride electrolytes. This led to ~70% improvement in the energy density compared to the single sulfate system.[27]

Two different types of the electrochemical cell (flow-by and flow-through) share the same basic design. Flow-through geometry, presented as schematic representation in Figure 2, is often used in industry and therefore the study in this thesis is based on this design. The cell consists of current collectors, mostly graphite-based plates, at the end plates, attached to carbon felts with different thicknesses, and separated by flow field, gaskets and cation or anion exchange membrane. The whole cell is usually compressed up to 50% to reduce contact

resistance.[28-29] However, the applied pressure can result in lowering the porosity of the felts leading to increased pressure drop and therefore the applied compression should be optimized.[30]

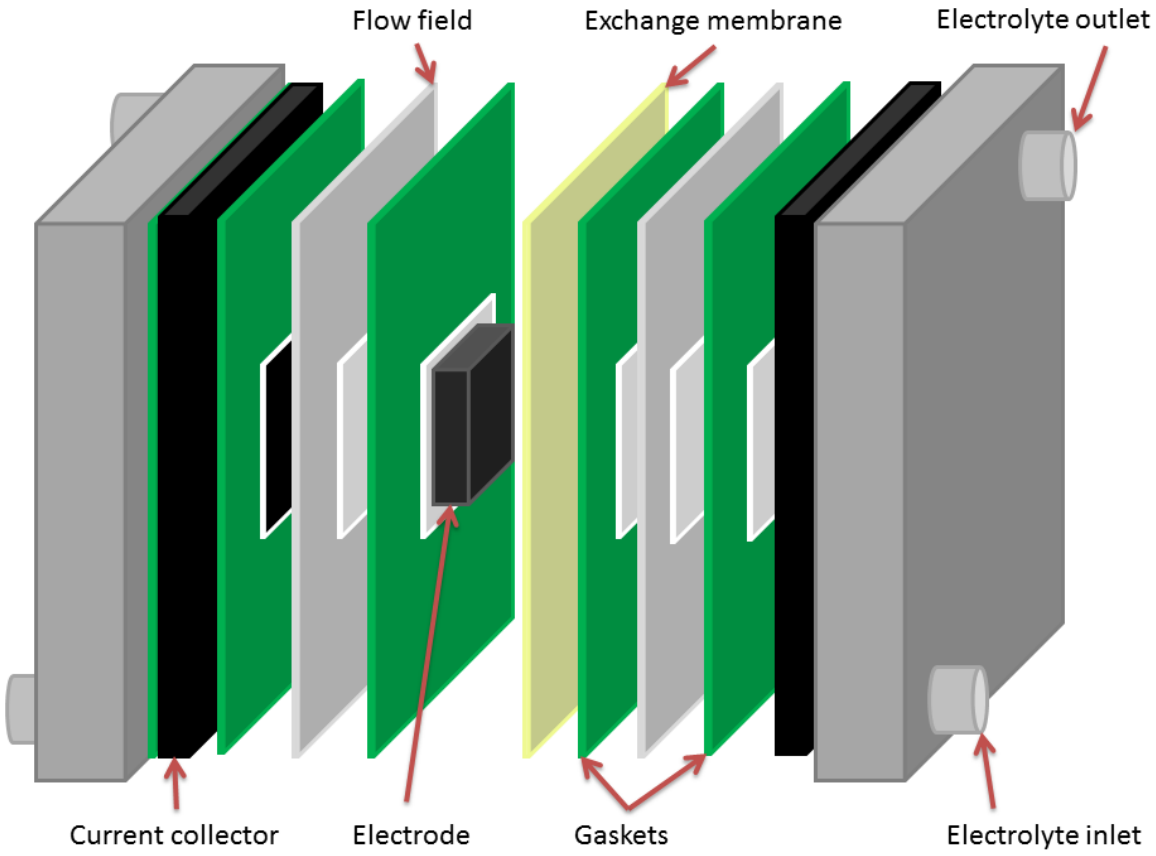

Figure 2: Schematic representation of flow-through geometry cell used in VRFBs.

Graphite plates are the standard material used as current collector in VRFBs. In single and multiple cell-stacks the use of carbon-based bipolar plates is highlighted in the literature to provide the electrical conductivity and physical separation of adjacent cells and prevent leakage of electrolyte.[31-32] The plates should be chemically stable in the highly acidic environment inside the electrolyte and have a good corrosion resistance during overcharge at the positive electrode.[33] Bipolar plates are usually prepared by combining conductive carbon materials, such as carbon blacks, graphite or carbon nanotubes, with binders, like polyethylene, polypropylene, polyacrylonitrile or epoxy resin, to form carbon-filled materials.[34-40]

The proton exchange membrane is one of the important and expensive parts of VRFBs,[19] the membrane is usually used to provide proton transport during the charge-discharge to complete

the circuit and to prevent cross-mixing of the positive and negative half-cell electrolytes.[41] A suitable membrane should possess low permeability of vanadium ions, low resistivity and good chemical stability.[42] An increased rate of cross-over of vanadium through the membrane will result in an increased rate of self-discharging, electrolyte imbalance and loss in coulombic efficiency.[43-46] Few expensive commercial membranes can meet the previously specified requirements, and therefore many researchers investigated the synthesis of cheaper composite membranes by different approaches and the modification of such alternative membranes to improve their performance.[47-53]

Electrodes are a key component in VRFBs; the electrodes are usually felts or papers consisting of few millimeters of carbon-based materials. The carbon felts or papers are textile materials of randomly oriented fibers synthesized from different precursors, mainly rayon and polyacrylonitrile (PAN). Thanks to their low cost, wide operating potential range and inertness in harsh acidic conditions those carbon materials are frequently reported as best choice for electrodes in VRFBs application.[54-55] However, pristine carbon felts normally exhibit poor electrochemical activity and reversibility which limit the voltage efficiency and power density of VRFBs. Many studies have been reported to enhance the wettability and electrochemical properties towards both the V(II)/V(III) and V(IV)/V(V) redox couple, e.g. thermal treatment,[10, 56] acid treatment,[8-9] deposition of noble metals[57-59] and metal oxides[14, 60-62] on the surface of the electrodes. However, despite the improvement of the performance using these techniques, which are considered simple and fast for improving the electrochemical activity of CF electrodes, the obtained improvement was rather limited[63] and the felt's long-term stability after treatment has not been studied in detail.

In an operating VRFB cell a specified potential window is set and the cell is charged\discharged between these two reversal potentials. The two potentials (0.8 V in the discharge process and 1.8 V in the charging process), called cut-off voltages, are chosen to utilize the maximum theoretical capacity and efficiency. Exceeding the maximum potential of the charging process can result in parasitic reactions, for instance, oxygen evolution\carbon oxidation in the positive half-cell and hydrogen evolution in the negative half-cell.[64-67] Operating the cell at higher current density involves higher overpotentials leading to lower energy efficiency (EE) (eq. 3) of the system, a value which consists of coulombic efficiency (CE) (eq. 4) and voltage efficiency (VE) (eq. 5).

$$EE = CE \times VE \quad (3)$$

$$CE = \frac{\int I_{discharge}\, dt}{\int I_{charge} dt} \quad (4)$$

$$VE = \frac{\int U_{discharge}\, dt}{\int U_{charge}\, dt} \quad (5)$$

The previous two efficiencies depend on operating conditions in either a direct or an indirect way. The coulombic efficiency is strongly affected by the cross-over of vanadium through the membrane during cycling, oxidation of V(II) to V(III) in the negative half-cell and the parasitic reactions, mainly the hydrogen evolution reaction (HER) during the charging process. The cross-over of vanadium could be minimized by the choice of membrane. Unwanted oxidation of V(II) to V(III) with atmospheric oxygen is prevented by an inert gas blanket (e.g., N_2, Ar). While the electrode surface determines which reaction takes place, at higher current densities, elevated temperatures and in mass transport limited regimes the HER becomes favored compared to vanadium reduction, an issue which results in self-discharge and an imbalance of the electrolyte and therefore a decreased coulombic efficiency.[2, 68]

The voltage efficiency depends on concentration overpotentials, ohmic overpotentials and ionic overpotentials. The concentration overpotential is generated due to different concentrations of electroactive species between the bulk solution, diffusion layer and reaction layer close to the electrode surface where the electron transfer occurs (see Figure 3). In order to keep the current steady, the rate of mass transfer from the electrolyte to the electrode surface should be increased and fresh reactants must be continuously introduced to the reaction layer from the bulk of the electrolyte. The ohmic overpotential is caused by the electron conduction in carbon felt electrodes, current collector plates and within the connecting wires. Ionic overpotential is caused by flow resistance of an ionic current in the electrolyte and the membrane. [69] Therefore, cautious selection of the cell's components could lead to higher performance. Nevertheless, an energy efficiency below 85% is usually reported for VRFB systems[6, 20] due to the previous overall losses, slower kinetics of the VO^{2+}/VO_2^+ couple compared to V^{3+}/V^{2+} couple and the voltage losses during the discharge process associated with the slower reduction of VO_2^+ in contrast to the oxidation of VO^{2+}.[70]

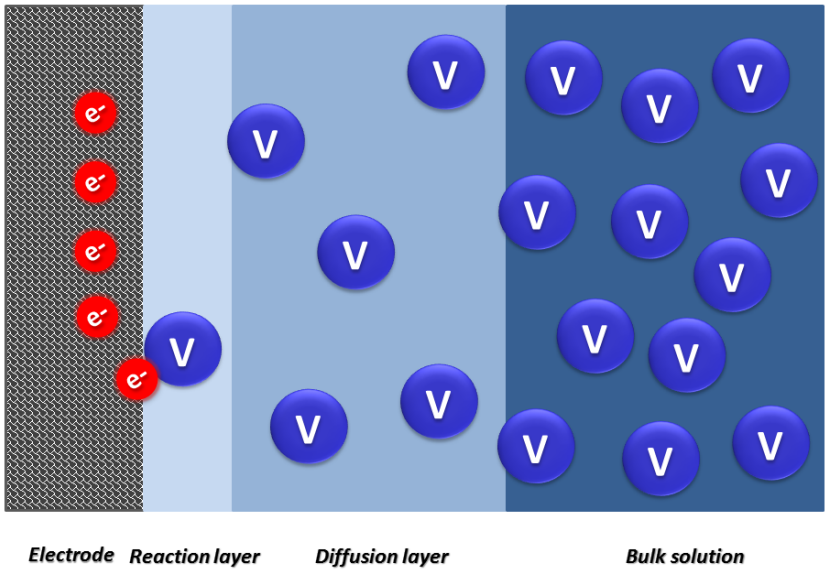

Figure 3: Concentration differences in the different layers of electrolyte.[69]

1.2. Carbon fibers as electrode materials

Carbon based electrodes are widely used in electrochemical applications due to their good electrical conductivity and chemically inert behavior. Moreover, the inexpensive manufacturing costs compared to alternative electrode materials such as precious metal electrodes, in addition to adaptable morphology and capability of change in surface chemistry which can greatly influence its electrochemical behavior, make them a favorable choice.[68, 71-72]

The synthesis of carbon fibers' from rayon was patented in 1959 by Ford and Mitchell. The process is based on heat-treatment of rayon to high temperatures up to 3000 °C. Meanwhile, the use of PAN as a precursor of carbon fibers has been developed by European and Japanese scientists at the same time.[73]

Carbon fibers are being utilized in many applications, such as in the defense industry, automotive industry, sporting goods, musical instruments and energy storage devices. Commercial carbon fibers are non-woven felts made of PAN, pitch or cellulose. Fibers based on PAN are the most widely used in the field of VRFB.

The synthesis of PAN-based carbon fibers consists of mainly two steps; thermal stabilization as the first step which is usually carried out in air where the fibers are stretched and oxidized by heating to temperatures between 200-300 °C. Three reactions (oxidation, dehydrogenation and cyclization) are involved in this step where thermoplastic PAN fibers are converted to

thermally stable ladder-like PAN compounds (see Figure 4). In this step, in addition to the incorporation of oxygen, a ring closure of the nitrile groups to a polyimine-like structure takes place. This facilitates the crosslinking of the polymer during the subsequent carbonization step and thus the formation of graphitic basal planes. In the dehydrogenation reaction, water elimination occurs and lastly the triple bond structure is converted to a double bond one in the cyclization reaction, substituting the aliphatic structure to cyclic structure and resulting in the six-membered cyclic ring (see Figure 5).[74-76]

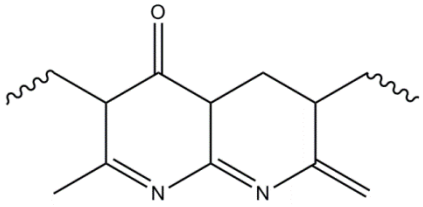

Figure 4: Ladder-like PAN structure.[76]

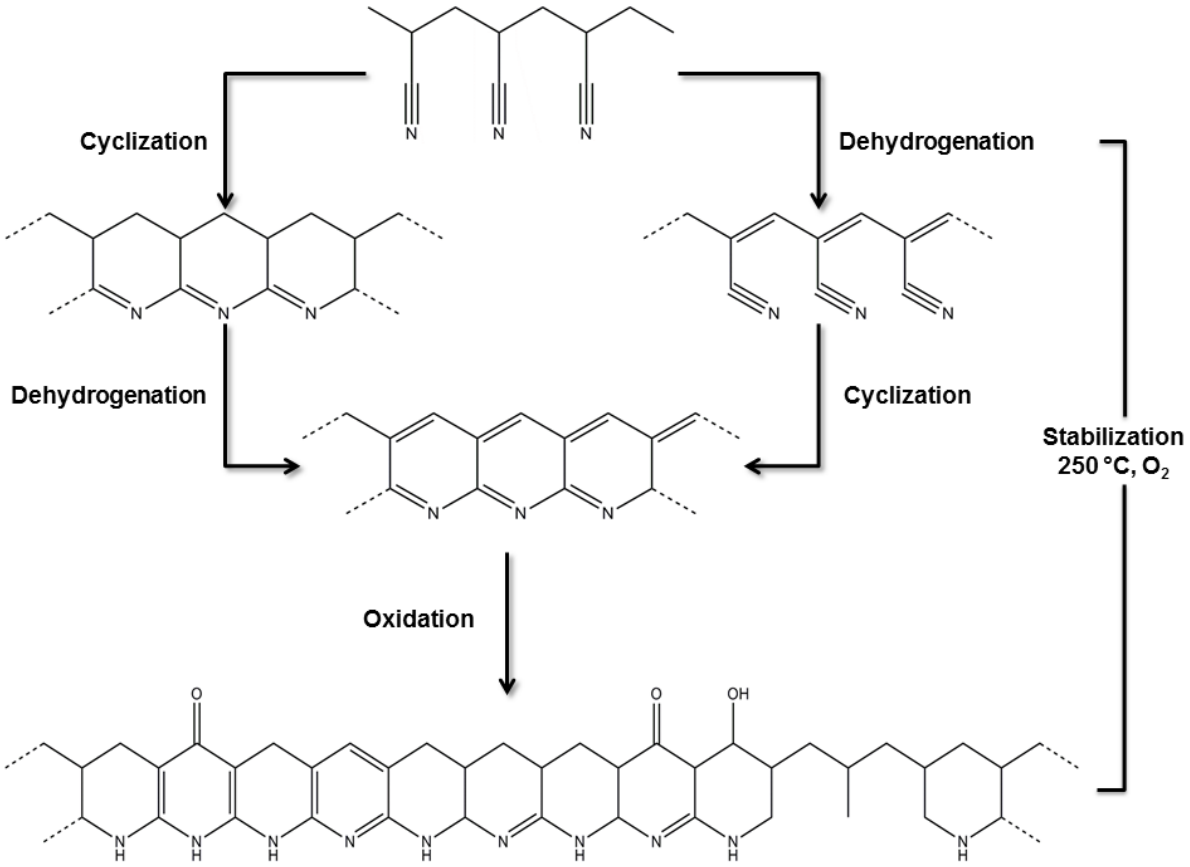

Figure 5: Proposed chemistry of stabilization reactions of PAN.[76]

The second step is carbonization which is usually carried out in the range of 1000-1100 °C in an oxygen-free environment where around 95% carbon content is achieved and non-carbon impurities, such as nitrogen and hydrogen, are removed by intermolecular crosslinking of the

polymer chains and the dehydrogenation reactions (see Figure 6). The carbonization step may be followed by the additional step of graphitization; this step stretches the fibers between 50 to 100% elongation in an inert atmosphere and high temperatures ranging from 2000 °C to 3000 °C.[74-76]

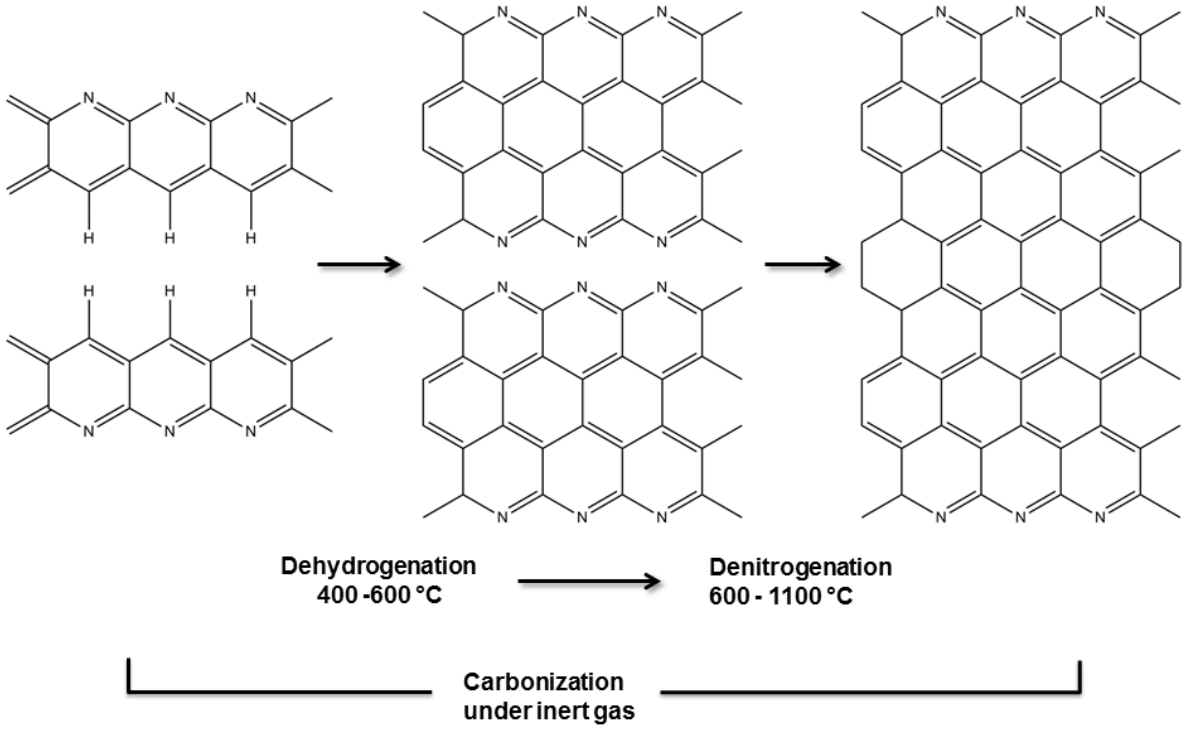

Figure 6: Schematic representation of the formation of graphitic structures by carbonization of PAN.[76]

1.3. Electrospinning

The synthesis and fabrication of one-dimensional nanostructures has been studied intensively. Among many approaches, electrospinning was found to be a simple technique for producing nanofibers which have uniform diameter, long length and various compositions.[77] Using a polymer solution or melt nanofibers are produced by electrospinning based on uniaxial elongation of a viscoelastic jet. A schematic illustration and a photo of the basic setup for electrospinning are presented in Figure 7. The simple setup usually consists of a power supply for high voltage connected to a spinneret (metallic needle) at one end and a collector at the other end. The polymer solution or melt is provided to the system with controlled and constant rate by means of a syringe pump. The applied high voltage will electrify the suspended drop of the polymer solution at the end of the needle where a Taylor cone is

formed that spreads charges over the surface of the suspended drop. As a result, the polymer jet will suffer instabilities due to following major types of forces:

I) The electrostatic charge repulsion between surface charges and the coulombic forces introduced by the electric field, which destabilizes the jet and increases its surface.

II) The surface tension, which tends to stabilize the jet by minimizing the surface. [77-78]

Increasing the electric field, until a threshold value is obtained, will favor the repulsive electrostatic forces to overcome the surface tension and thus force the ejection of the charged jet from the tip of the needle.[79] The jet then suffers from stretching and elongation leading to long and very thin strings with a diameter that has been reduced from hundreds of micrometers to tens of nanometers. Meanwhile, the solvent evaporates, leaving behind a charged polymer fiber. The fibers are usually collected in random non-woven order on the collector. This simple technique can be applied over more than fifty different organic polymers producing fibers with different diameters depending on the application.[77, 79-81]

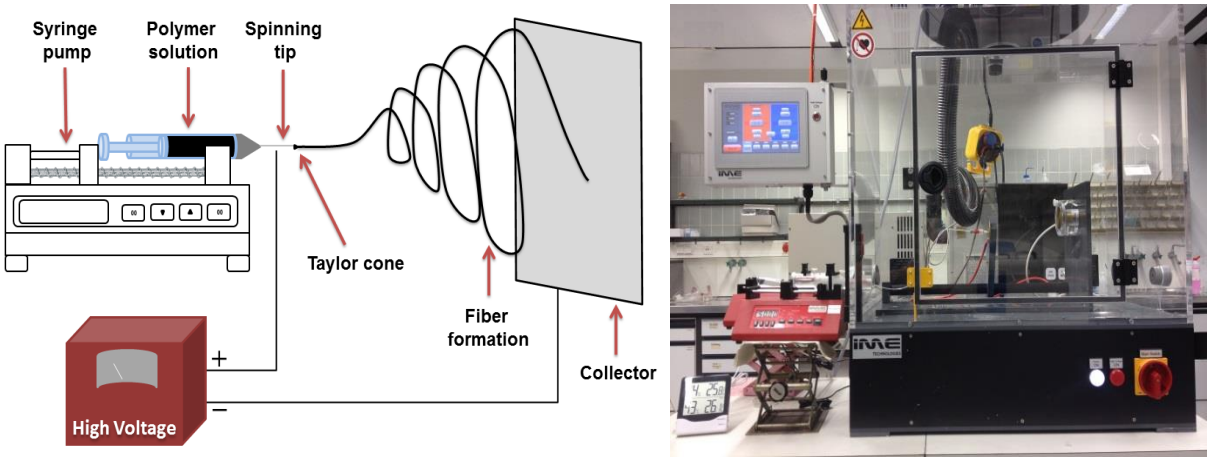

Figure 7: Left: A schematic representation of the basic setup of electrospinning, right: photo of the real setup.

The electrospinning process is influenced by many parameters. These parameters include (i) the solution properties such as concentration, viscosity, conductivity, molecular weight of the polymer, and surface tension, (ii) ambient related parameters such as humidity, temperature, and air velocity in the electrospinning chamber and (iii) other variables, such as electric potential at the spinneret, flow rate, and the distance between the spinneret and the collector.[79, 82]

Even though electrospinning is considered a simple technique, the productivity of the process is still low (feed rate less than 1 mL/h) and the resultant fibers have non-woven entangled structure. However, many researchers tried to increase the low feed flow rate by modifying the setup in a number of ways. For instance, some of them have used a capillary-less rotating charged electrode cylinder, where the solution is pushed by air pressure, or splashing a solution onto the surface of a metal roller spinneret connected to a positive high voltage.[83-84] Other researchers reported new ways to tailor the resulting structure by introducing rotating drums, collectors based on split electrodes and dielectric plates with sharp pin electrodes to collect the fibers in relatively uniform mats.[85-88]

The produced electrospun fibers could be modified in many ways to broaden their features and improve their performance. For example, electrospun nanofibers could be loaded with metal nanostructures via a simple strategy including electrodeposition or chemical techniques and such fabricated metal-decorated nanofibers are holding much promise for the use in many potential applications such as catalysis and fuel cells.[89-91] Other studies demonstrated fabrication of composite fibers with noble metal nanoparticles with controlled size and density of the deposited metal nanoparticles and non-precious metals or carbon materials.[92-94] Recent literatures investigated the production of core/shell fibers by co-electrospinning of two different polymers solutions through two coaxial capillaries and hollow nanofibers by merging oil to the interior structure of the fibers.[95-99]

1.4. Thesis outline and research objective

This thesis is written in a cumulative way. The four peer reviewed articles are supposed to give an insight into the results that were obtained within this Ph.D. project.

The main objectives were:

- Synthesis of electrospun carbon nanofibers
  - Develop reproducible recipe of composite electrospun materials
  - Optimize electrospinning parameters
  - Define carbonization procedure of electrospun fibers

- Characterization of carbon fibers
  - Find suitable measurement techniques
  - Analyze data and compare with commercial carbon felts

- Correlate the kinetic parameters to surface properties of the produced carbon fibers

- Investigation of the electrodes degradation by parasitic side reactions
  - Correlate the effect of environmental conditions to the cell performance
  - Find suitable measurement techniques

- Implementation of fabricated/modified felts in vanadium redox flow system
  - Develop reproducible protocol for testing the performance of the materials
  - Set evaluation parameters for comparison between felts
  - Investigate the stability of the fabricated/modified felts

The main objective of this work was to develop a reproducible synthesis and/or modification strategies for carbon-based fibers and integrate these fabricated materials into the real VRFB system. Besides, both the performance and the degradation of the as-prepared materials have been correlated to their morphology, composition and internal structures using different microscopic, spectroscopic and diffraction techniques.

2. Methods and techniques

2.1. Three electrode half-cell set-up

The electrochemical activity of the carbon materials was characterized in this work by cyclic voltammetry (CV) and electrochemical impedance spectroscopy (EIS) measurements. A three-electrode setup consisting of working, counter and reference electrodes was used (see Figure 8). The reactions under investigation occur at the working electrode. Therefore, it consists of the material to be examined and a holder (glassy carbon is used) which is electrically conductive, but electrochemically inactive. The reference electrode serves as a zero-point potential, to which the potential difference is related. In this thesis, saturated calomel electrode (SCE) was used, it has a potential of +0.248 V versus standard hydrogen electrode (SHE) under standard conditions.

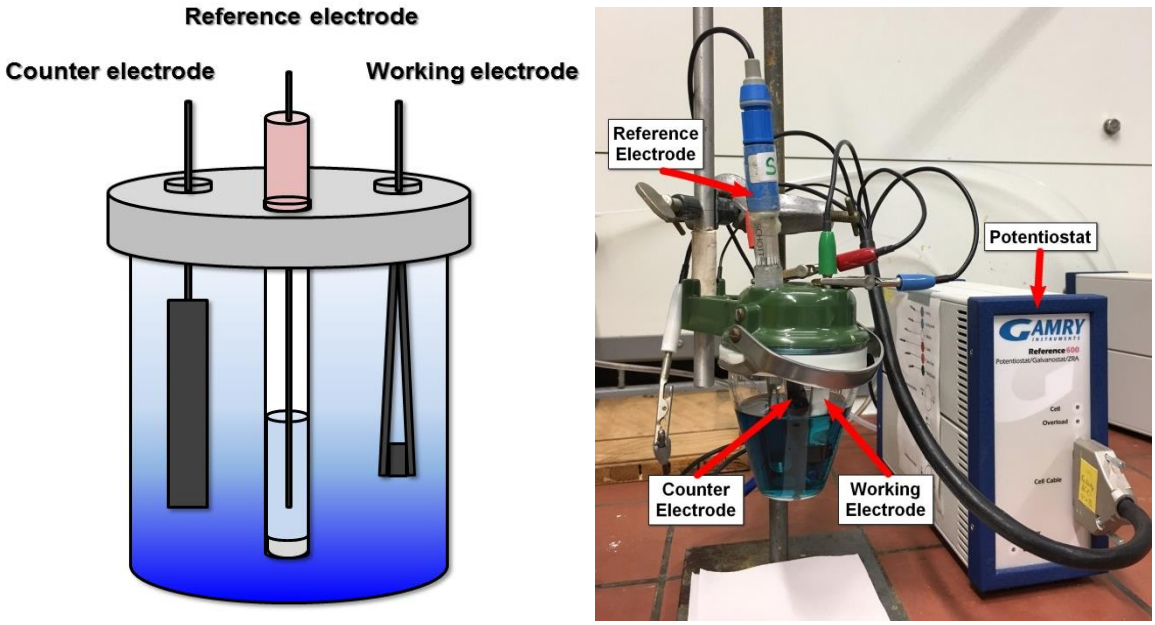

Figure 8: Left: Schematic illustration of the three-electrode arrangement; Right: photo of the setup.

2.1.1. Cyclic voltammetry

In cyclic voltammetry, the potential of the working electrode is measured against a reference electrode which maintains a constant potential, the working electrode potential is then ramped linearly versus time until it reaches a set potential sufficient enough to cause an oxidation or reduction. The reverse scan occurs when the potential is inverted using a triangular potential waveform (Figure 9). The slope of the excitation signal gives the scan rate (V/s). This cycle can be repeated multiple times in a single experiment. A cyclic voltammogram is obtained by measuring the current during potential scan.

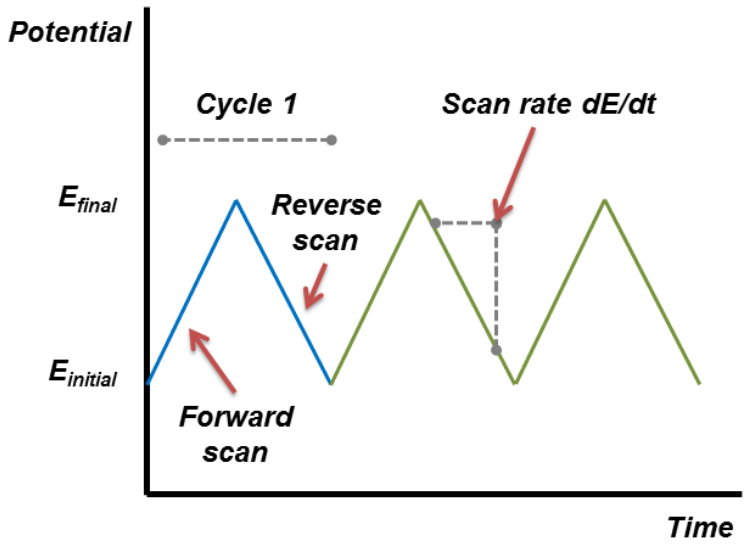

Figure 9: Potential-time response signal in cyclic voltammetry experiment.[100]

As the potential is scanned positively from point A to point C (Figure 10) anodic current starts to appear when the applied potential approaches $E°$ for the redox process, V(IV) is steadily depleted near the electrode and oxidized to V(V), the current is increased reaching a maximum where a peak could be observed. At point B, where the peak anodic current ($i_{p,a}$) is observed, the current is dictated by the delivery of additional V(IV) via diffusion from the bulk solution. The diffusion layer continues to increase throughout the scan. This results in slowing down mass transport of V(IV) to the electrode. Thus, upon scanning to more positive potentials, the rate of diffusion of V(IV) from the bulk solution to the electrode surface becomes slower, resulting in a decrease in the current as the scan continues. After passing the potential region where the oxidation could occur, the potential ramp is inverted and the oxidized molecules produced in the first half cycle and close to the electrode surface will be reduced resulting in a cathodic peak ($i_{p,c}$).[101] The evaluation of CV results usually depends on different parameters, such as the peak current, the peak position, the onset potential and peak separation. The peak current, the peak position and peak separation significantly depend on the electrochemical surface area (ECSA) and also on the mass-transport and diffusion. In 3D structure thick electrodes with different pore size, mass-transport and diffusion inside the felt become a considerable issue, especially in the case of bulky felts where convection through the felt even by using a magnetic stirrer is negligible, the electrolyte inside the felt is exchanged only by diffusion during the measurement. In addition, the vanadium reaction is a quasi-irreversible reaction, which will influence the peak position and the peak current in a CV measurement.[102] The evaluation of the CV measurements is usually based on some important parameters such as, i) peak current and the ratio of observed peak currents on the forward and reverse scans, both peak currents should be equal if the product is stable on the time scale of the experiment, ii) the onset potential, which is the starting point of the reaction and iii) peak separation (ΔE) described as the difference between the anodic and cathodic peak potentials, where an observed increase of ΔE when increasing the scan rate indicates the presence of electrochemical irreversibility. An active sample would be characterized by high peak current, low peak separation or early onset potential.

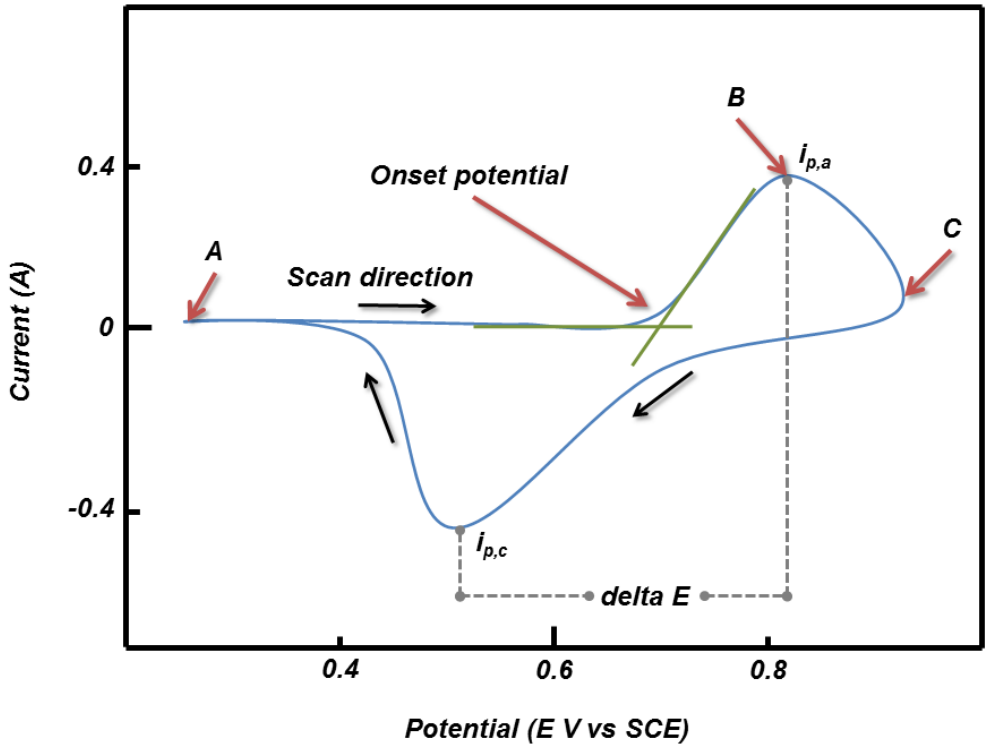

Figure 10: Typical CV of the positive half-cell and the analysis of the significant parameters.

2.1.2. Electrochemical impedance spectroscopy

Electrochemical impedance spectroscopy is a powerful diagnostic tool that can be used to characterize limitations and improve the performance of the redox flow battery. In EIS measurement an excitation voltage of specific amplitude is applied at a certain potential (e.g. state of charge 50%) over a certain frequency range. The excitation signal is expressed as a function of time in the form:

$$E_t = E_0 \sin(\omega t) \qquad (6)$$

The response current signal is shifted in phase (φ) and has different amplitude than I_0:

$$I_t = I_0 \sin(\omega t + \varphi) \qquad (7)$$

The impedance of the system which is the correlation of voltage input and responding current then could be calculated as:

$$Z = \frac{E_t}{I_t} = Z_0 \frac{E_0 \sin(\omega_t)}{I_0 \sin(\omega_t + \varphi)} \qquad (8)$$

The impedance is therefore expressed in terms of a magnitude (Z_0), and a phase shift (φ). Using Euler's relationship, the impedance can be represented as a complex number:

$$Z = \frac{E}{I} = Z_0 e^{j\varphi} = Z_0(\cos(\varphi) + j\,sin(\varphi)) = Z_{real} + j\,Z_{im} \qquad (9)$$

Where (φ) is real number and (j) is imaginary unit, EIS data may be presented as a complex plane so-called Nyquist Plot (Figure 11). In such plot, a phase shift of 0° describes an ohmic behavior (Z_{real}) and a phase shift of -90° describes pure capacitive behavior (Z_{im}).

Executing EIS measurements on fresh and aged carbon felts can provide valuable information about the contact resistance R_u and charge transfer resistance R_{ct} giving reliable results on the degradation progression of the carbon felts during the charging/discharging process.

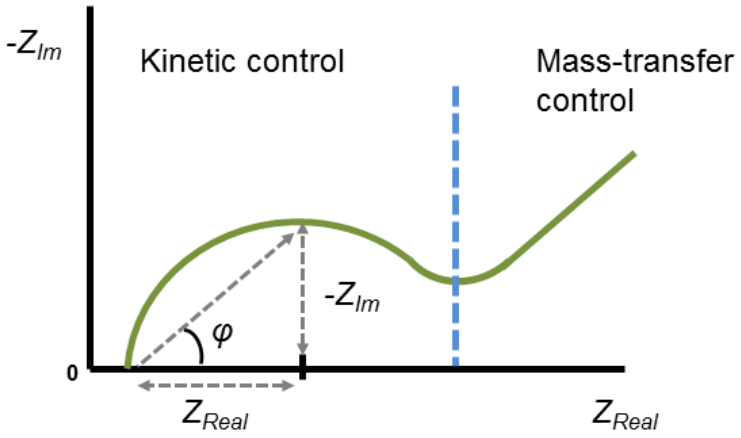

Figure 11: Impedance data represented as a Nyquist plot.

2.2. Characterization techniques

2.2.1. Raman spectroscopy

Raman spectroscopy is one of the vibrational spectroscopic techniques used to provide information on the crystalline perfection of graphite-based materials. A laser light source is used to irradiate a sample, and generates Raman scattered light which is detected by a CCD camera. Raman scattering occurs when incident light interacts with molecular vibrations. Even though most of the light which is scattered is unchanged in energy (Rayleigh scattering), a very small percentage of scattering is generated in an inelastic process which has lost or gained energy (Raman scattering). This Raman shift occurs because photons exchange part of their energy with molecular vibrations in the material.[103] Raman scattering is usually categorized into two types. The first, when an electron is excited from the ground vibrational

state and falls to a higher energy excited vibrational state the Raman scattering is designated as Stokes scattering, the scattered light has less energy (longer wavelength) than the incident light. And the second, when an electron is excited from a higher energy excited vibrational state to the ground state, the Raman scattering is designated as anti-Stokes scattering, the scattered light has more energy (shorter wavelength) than the incident light (see Figure 12). The relative intensities of the two processes depend on the population of the different states of the molecule. At room temperature, the number of molecules in a high energy excited vibrational state is expected to be smaller than that in the ground state. Thus, the intensity of Stokes scattering is higher than anti-Stokes scattering.[103] In a typical Raman spectrum of a carbonaceous sample (Figure 13), material specific vibrational modes of molecular functional groups can be identified by peak position and relative intensities. Crystallinity and stresses inside the sample can be derived from the width of the peak or the direction and amount of shift of the Raman peak.

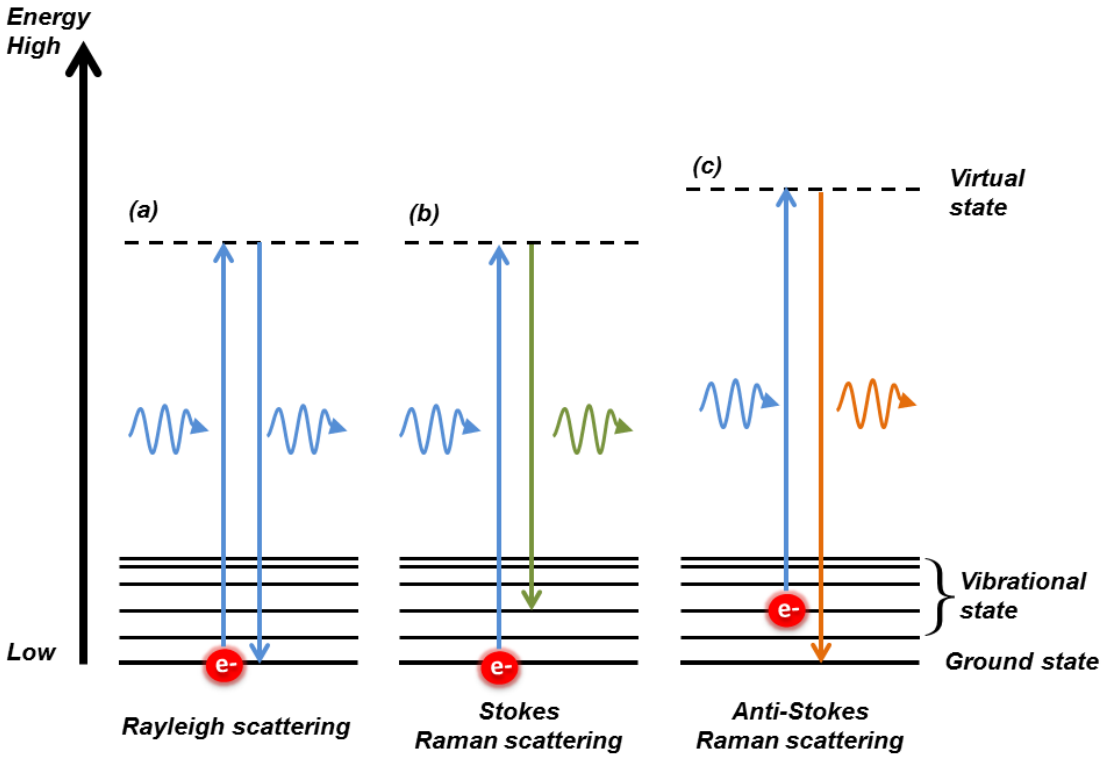

Figure 12: Rayleigh and Raman scattering energy diagram (a) energy is unchanged. (b) energy is lost (c) energy is gained.[103]

The Raman spectra of carbonaceous materials mainly consist of two modes; the G mode (graphene like structure) describes the primary in-plane vibrational mode and the D mode (diamond like structure) describes the disordered structure of graphene. The R value (the intensity ratio of I_D/I_G) is often used as an indicator of the graphitization degree of a sample.

The first order D and G modes are usually fitted by five peaks. The G band at ~1580 cm^{-1} is assigned to "in-plane" carbons strongly coupled in the hexagonal sheet. The D band can be fitted by four peaks, where D1 at ~1350 cm^{-1} and D2 at ~1600 cm^{-1} are assigned to disorder in the structure, whereas the D3 at ~1500 cm^{-1} is assigned to amorphous sp^2-bonded carbons or interstitial defects and D4 at ~1200 cm^{-1} is assigned to sp2–sp3 bonds or C-C and C=C stretching vibrations of polyene-like structures.[104]

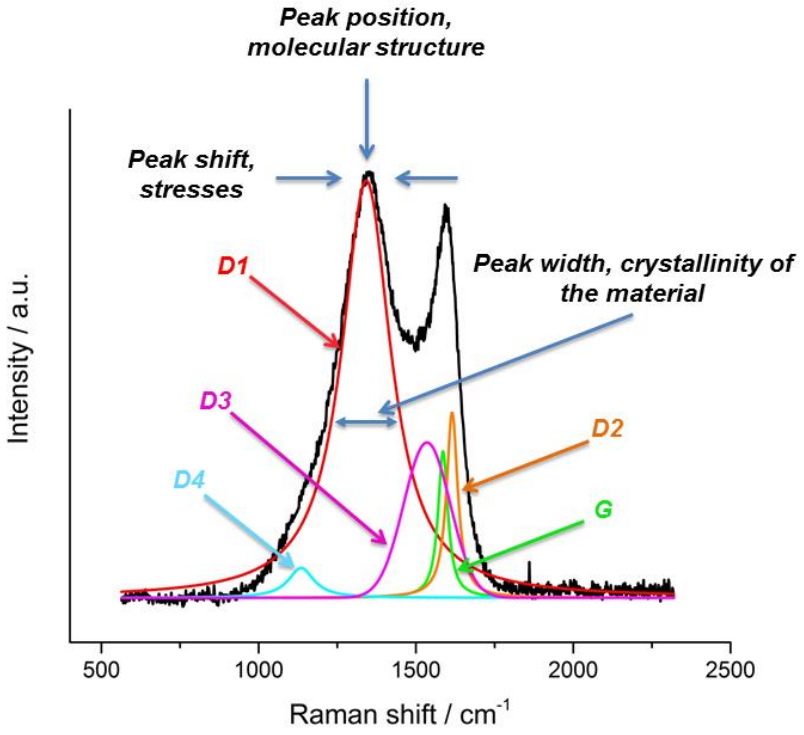

Figure 13: Typical Raman spectrum of carbon felt.

2.2.2. X-ray diffraction

X-ray diffraction (XRD) is a non-destructive technique for analyzing the crystalline structure of materials. A beam of X-rays is generated by a cathode ray tube, filtered to produce monochromatic radiation, concentrated and then directed towards a sample, and the scattered intensity is measured as a function of outgoing direction. Constructive interference is observed when the conditions of interactions of the incident rays with the sample satisfy Bragg's law (eq. 10). The diffracted X-rays are then detected, processed and counted.

$$n\lambda = 2\,d\sin\theta \qquad (10)$$

Bragg's law relates the wavelength of electromagnetic radiation (X-rays beam) λ to the diffraction angle between the incoming and outgoing beam 2θ and the lattice spacing d in a crystalline sample. All possible diffraction directions of the lattice can be obtained by scanning the sample through a range of 2θ angles. Conversion of the diffraction peaks to *d*-spacing allows identification of crystalline solid phases, e.g. minerals, in the sample; this is achieved by comparison of *d*-spacing with standard reference patterns. The investigated material is usually evident by characteristic peaks which correspond to reflection planes. The presence of such peaks in the reflection pattern can provide a qualitative detection of the material and the shape of those peaks can provide information about the crystallinity of the material (for instance, more intense peaks means higher crystallinity) and size of particles (FWHM-broadness of peaks). In carbons, the main focus of analysis is on the C (002) reflection: the higher and narrower the peak, the more crystalline the carbon. This can also be used as an indication for degree of graphitization.

2.2.3. X-ray photoelectron spectroscopy

X-ray photoelectron spectroscopy (XPS) is a surface-sensitive quantitative spectroscopic technique that can be applied to a broad range of materials to measure the elemental composition and provide valuable quantitative and chemical state information of the elements that exist in a material. The XPS spectrum is obtained by scanning a micro-focused X-ray beam across the sample surface while simultaneously measuring the kinetic energy and number of electrons that is emitted from the top 5 nm of the surface of the sample. Therefore, this technique is suitable to analyze the surface properties of carbon materials. Figure 14 shows an example of an XPS spectrum and the binding energy region of the carbon 1s orbital of a carbon felt. A prominent way of analyzing surface layer compositions of carbon materials is the sp^2/sp^3 hybridization ratio and the characteristic binding energies of surface functional groups, such as C=O, C-OH and COOH. These functional groups are claimed to be active towards catalyzing the negative and positive half-cell reactions, but also important to the wettability properties.

Electron transport in carbon materials is mainly facilitated by the π-orbital of sp^2 hybridized carbon; a decreased amount of sp^2 carbon will result in lowering the conductivity of the CF and therefore limits the charge transfer process. An increase in the oxygen functionality content on the carbon surface will increase the hydrophilicity and simultaneously increase the active sites. However, a balance between the oxygen functionality content and sp^2 hybridized

carbon is believed to be necessary to demonstrate good kinetics and stability of the carbon felts.

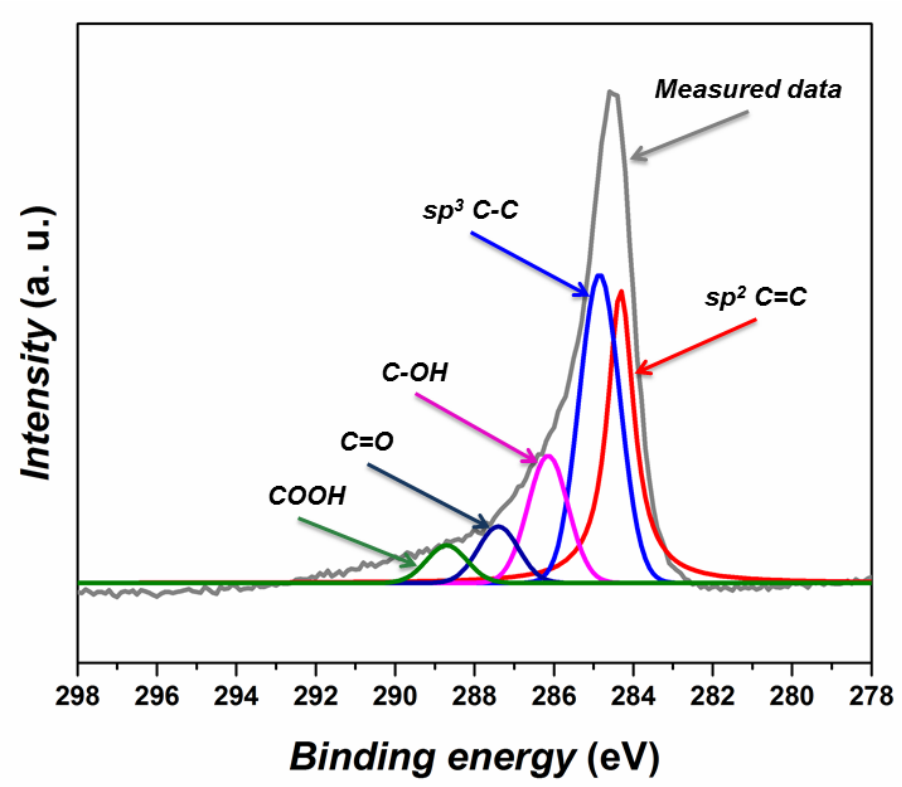

Figure 14: Example XPS of pristine commercial carbon felt.

2.2.4. Scanning electron microscopy & energy-dispersive X-ray spectroscopy

Scanning electron microscopy (SEM) is a powerful and versatile tool which is usually used to investigate the morphology of surfaces and electrical behavior of the sample. This technique has many advantages, such as the capability of scanning large samples size, simple preparation procedure and the ability of non-destructive evaluation of the samples, which makes it one of the favorable techniques for characterization. In SEM, the images are produced by scanning the top (~1 μm) of the sample with a focused beam of high-energy electrons (2-40 keV) which is produced from an electron gun. The beam is focused on a selected area of the sample surface with electromagnetic condenser lenses. The penetration depth of the electrons in the sample depends on the electron energy, incidence angle and atomic mass. As the electron beam interacts with atoms at or near the surface of the sample, they produce secondary electrons (SE), backscattered high-energy electrons (BSE) and X-rays (see Figure 15) which can be detected by a variety of detectors. The signal from the detectors is linked to a monitor to represent the image.[105-106]

The maximum resolution achieved in an SEM depends on many factors, for instance, electron spot size and interaction volume of the electron beam with the sample. While it cannot provide atomic resolution, modern scanning electron microscopes typically provide resolutions between 1-20 nm.

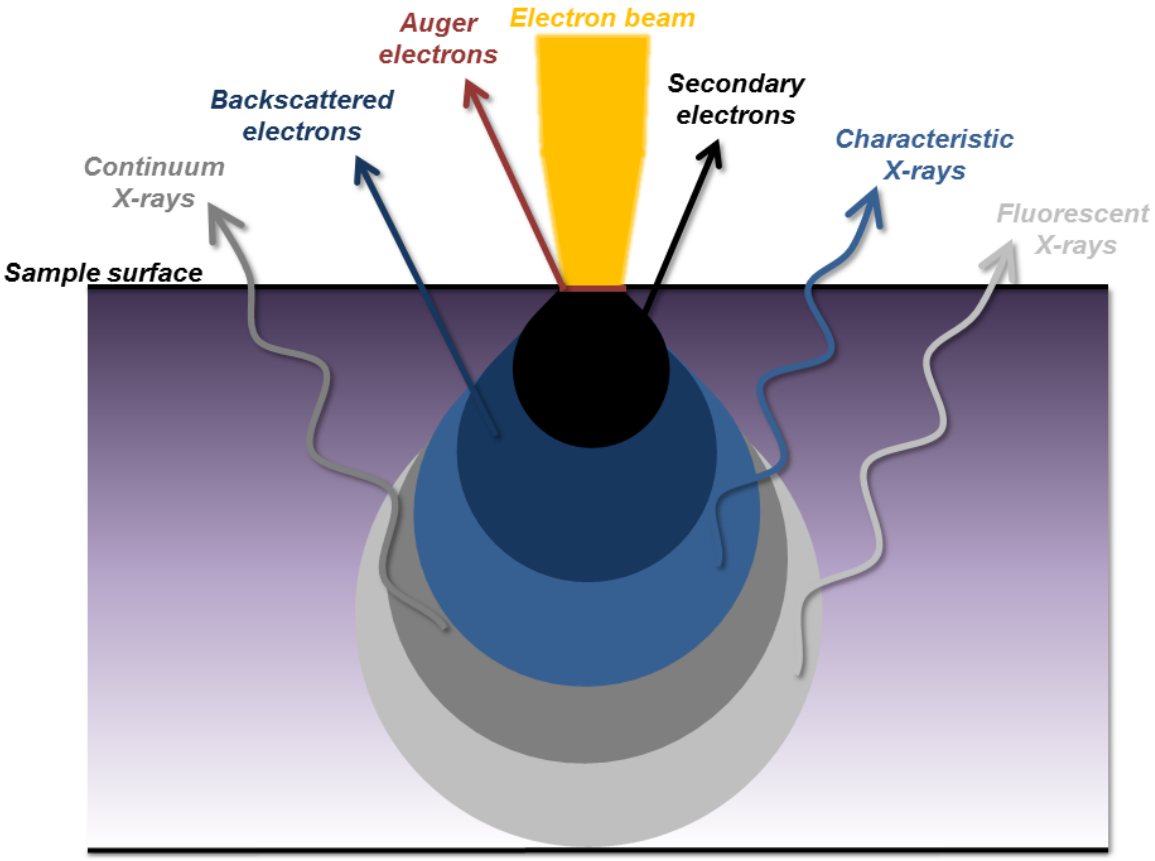

Figure 15: Schematic of electron interaction with matter.

Scanning electron microscopy is also capable of performing analyses of selected locations on the sample; this approach is called energy-dispersive X-ray spectroscopy (EDX), a useful technique for qualitatively or semi-quantitatively determining chemical compositions. The incident electron beam may eject an electron from the inner shell of the atom by exciting it; this will create an electron hole. A higher-energy electron from an outer shell then fills the hole, and the difference in energy between the higher energy shell and the lower energy shell is released as X-ray. The energy of the X-rays emitted from a sample can be measured by an energy-dispersive detector which contains a crystal that absorbs the energy of the incoming X-rays and produces an electrical charge pulse. The charge pulse is converted to a voltage pulse and the pulses are sorted by voltage. The voltage measurements of each X-ray are sent

to computer software for further data processing. The spectrum of X-ray energy versus counts can be evaluated to determine the different composition of different elements in the sample.[107]

The morphology of the carbon felts, the diameter of the fibers and the presence of beads generated in an electrospun sample can be easily accessed using SEM, while the presence and agglomeration of doped metal oxide and the elemental composition of doped felts can be examined using EDX.

2.2.5. X-ray computed tomography

X-ray computed tomography (XCT) is a non-destructive non-invasive technique for investigating the morphology of interior features of solid objects, and for obtaining digital information on its 3-D geometry and properties. In this technique, X-rays are generated by a micro-focus X-ray source, the X-rays are then pointed at the object and a planar X-ray detector collects 2-D X-ray images from various angular views acquired around an object while it rotates. After scanning, a computer is reconstructing digital three-dimensional stacks of virtual cross-sections through the object. Due to the relationship between X-ray absorption and material density, unique 3-D geometry representation can be derived from those slices.[108-109] The use of this technique facilitates the understanding of porous carbon materials structure in carbon felts and the detected 3-D geometry can be a dependable source to simulate the pore size distribution in the felts. An open source pore network modelling framework can then be utilized to calculate transport properties through the structure and simulate electrolyte flow through the carbon material to obtain a more detailed understanding of the electrolyte transport characteristics.

2.3. Redox flow cell test system

A lab scale redox flow test system is usually used to evaluate the performance of the cell equipped with different electrode materials. A test routine protocol is programmed in a way to help the assessment of the activity, stability and degradation of the felts and the effects of side reactions. In such a pre-set protocol the following sub-experiments are most likely to be used; charging and discharging cycles which highlight the activity and stability of the felt, polarization curves which could show a linear dependence of potential on applied current for small amounts of polarization, EIS and open circuit potential which can lead to the actual state of charge of the cell (an example protocol is highlighted in Figure 16). In order to perform individual half-cell measurements, two Ag/AgCl reference electrodes were

introduced at the inlet of each half-cell. In Figure 17 the setup with the reference electrodes at the inlets of the cell is shown.

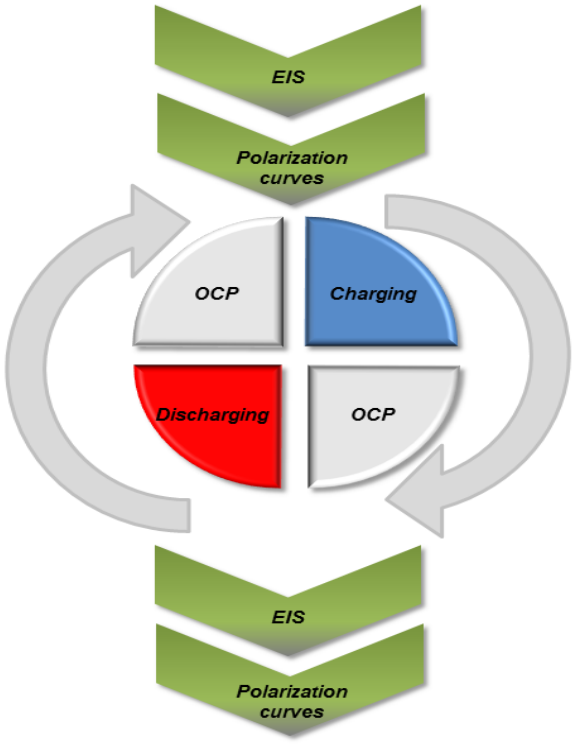

Figure 16: Example of testing protocol for redox flow test system

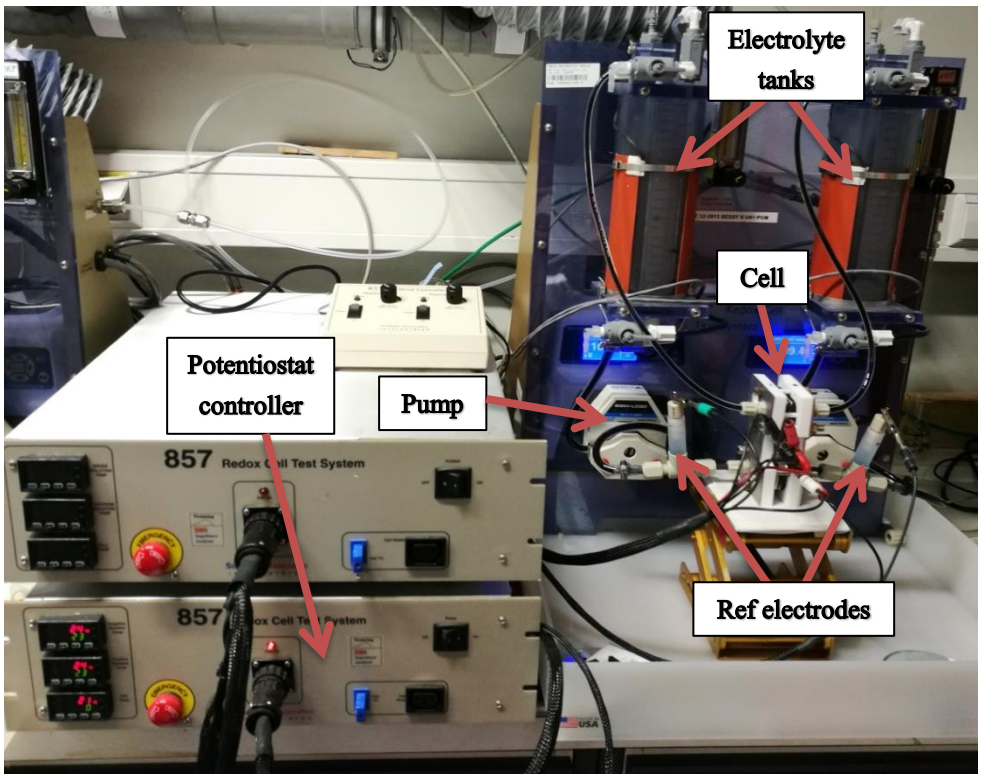

Figure 17: Redox flow test system with a flow cell and reference electrodes at the inlets.

3. Discussion of the scientific articles included in the thesis

The results and discussion of this thesis are organized in this chapter as four scientific articles as follows; fabrication of free standing carbon nanofibers web and their comparison to commercial carbon felts with respect to activity and stability was discussed in subchapter 3.1, the possibility of loading high amount of cheap carbon to the produced carbon nanofibers to reduce the cost of the materials and to enhance the activity and performance was investigated in 3.2. Exploring an alternative way for activating the commercial carbon fibers by neodymium oxide and enhancing their long-term stability is demonstrated in 3.3. In the last part of this work, the role of the parasitic hydrogen evolution side reaction and its temperature dependence and effect on the performance of the cell is discussed in 3.4.

3.1. Electrospun carbon nanofibers as alternative electrode materials for vanadium redox flow batteries

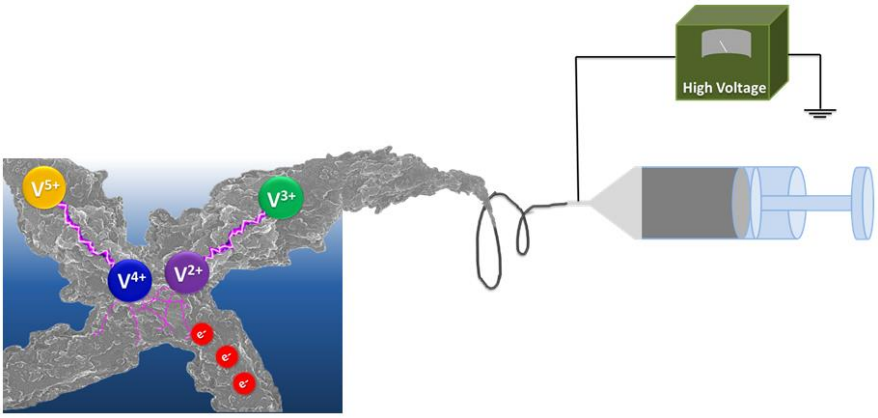

3.1.1. Motivation

Carbon felts (CFs) have been used as low-cost and stable electrodes since the beginning of RFBs. Many studies have been carried out to enhance the electrochemical activity, e.g. acid treatment, electrochemical activation and thermal treatment. The stability of the improvement obtained from such activation methods still suffer degradation over cycling and thus limits the voltage efficiency and power density of VRFBs during operation. Therefore, the development of innovative carbonaceous materials is in great demand. Only few scientific articles reported the preparation of carbon nanofibers (CNFs) with high surface areas by the electrospinning technique. Here, the synthesis of carbon-based nanofibers through electrospinning, forming a freestanding conductive network that can be used directly as an electrode in VRFBs, is highlighted.

3.1.2. Description and novelties

In this article, an electrospun polymer skeleton was prepared using PAN as a building unit for producing a non-woven web. The polymer structure was then stabilized and carbonized to produce high surface area active carbon nanofibers. BET analysis of the spun fibers showed higher surface area of almost 660 $m^2 g^{-1}$ compared to commercial carbon fibers (0.5 $m^2 g^{-1}$). SEM pictures of the electrospun carbon nanofibers (ES-CNFs) showed ultra-thin carbon fibers (~300 nm in diameter) which can be linked to the enormous surface area evident by BET analysis. The fabricated ES-CNFs were first tested in a three electrode setup where they showed promising results for the negative side reaction in VRFB. Five layers of the produced material were then tested as free standing electrode in the negative side in a real redox flow system at a current density of 15 mA cm^{-2} and showed promising results with an average energy density of 59% and discharge capacity of 1320 mAh for the first five cycles when compared to a commercial carbon felt with an average energy density of 49% and discharge capacity of 690 mAh. The fibers showed good mechanical stability during testing with no signs of fiber breakage evident in SEM after being compressed inside the battery hardware. The structure of ES-CNFs showed a less developed graphitic structure, but a higher fraction of more amorphous carbon due to the use of lower carbonization temperatures compared to CF as revealed by XRD and Raman spectroscopy.

3.1.3. Contribution

A. Fetyan: Shared idea, experimental work, writing and discussion, and publication

3.2. Comparison of electrospun carbon-carbon composite and commercial felt for their activity and electrolyte utilization in vanadium redox flow batteries

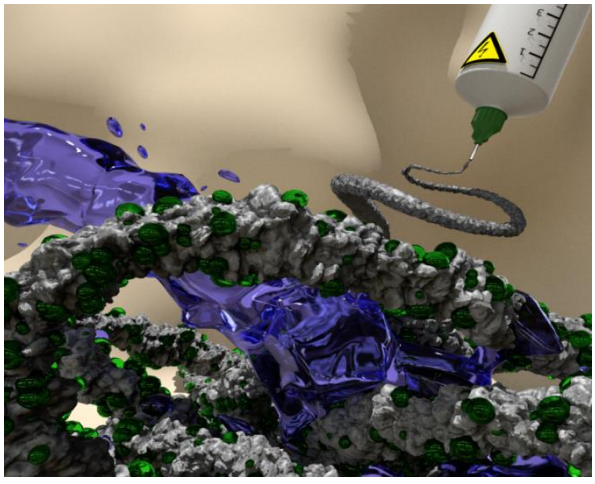

3.2.1. Motivation

Recent articles reported the use of PAN as carbon precursor for fabricating electrospun carbon nanofibers which can be used as supporting active layer in VRFBs. In the previous article, we highlighted the use of ES-CNFs as freestanding electrode in such batteries. However, VRFBs are still considered an overpriced technology compared to other available commercial systems, and consequently the use of PAN as the sole carbon precursor in electrospinning would add additional unwanted cost to the system. Adding a cheap alternative carbon precursor, which can enhance the activity of the fabricated material, is thus a highly desirable production route.

3.2.2. Description and novelties

PAN is considered one of the most suitable polymers in electrospinning producing carbon fibers in a facile manner. However, the uptake capacity of PAN is limited, so that an additional binder becomes necessary. Mixing PAN with PAA, more than 10 % (of the total weight of the mixture) of cheap carbon powder can be loaded into the polymer spinning solution. PAA will degrade at elevated temperatures during the carbonization step leaving a mixture of carbon-carbon (C-C) composite material. Three electrode setup static measurements indicated a significant performance increase for the C-C composite. However, the same performance could not be confirmed in the real redox flow system where the C-C composite showed a comparable performance to the commercial CF only at lower current densities (40 mA cm^{-2}). To fully understand the obtained data, the 3D structure of both samples was obtained by X-ray computed tomography. Pore network modeling showed smaller size of pores distributed between the fibers of the C-C composite than the one associated in commercial carbon felt (5-20 µm compared to 25-75 µm) which resulted in an increased capillary pressure and lower electrolyte invasion for the C-C composite material.

3.2.3. Contribution

A. Fetyan: Shared idea, experimental work, writing and discussion, and publication

3.3. A neodymium oxide nanoparticle-doped carbon felt as promising electrode for vanadium redox flow batteries

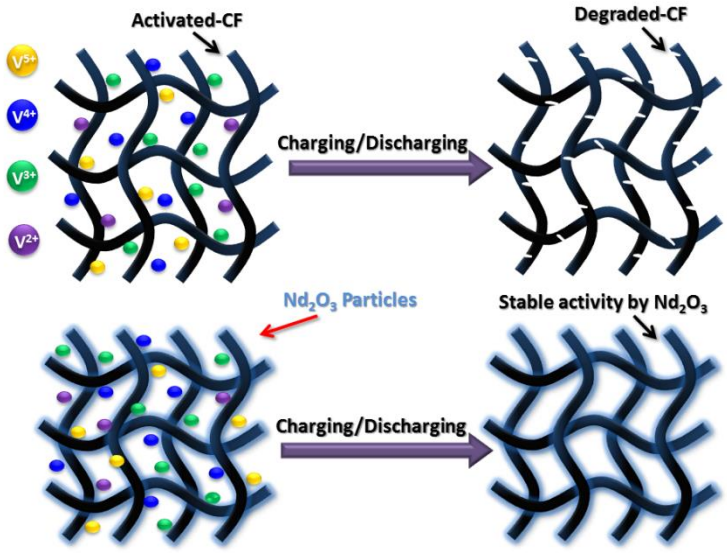

3.3.1. Motivation

Pristine carbon felts usually exhibit poor electrochemical activity toward redox reactions of vanadium. Among many surface modification methods to increase the performance of the fibers, thermal activation was found to be the easiest and most effective technique. However, recent studies reported degradation phenomena in the modified felts and highlighted the unknown long-term stability of this modification method. A new competitive approach to increase the electrochemical activity of the fibers in a sustainable way would be greatly appreciated.

3.3.2. Description and novelties

Neodymium oxide nanoparticles were chemically embedded by a precipitation method on commercial carbon felts. SEM and EDX mapping demonstrated a good dispersion of the oxide particles with almost no agglomerations. X-ray patterns were recorded and the reflections could be indexed to the characteristic Nd_2O_3 crystalline structure. Battery test results demonstrated a comparable performance of the modified felts to thermally activated felts in the first few charging/discharging cycles. The fade in activity of thermally activated felts was evident after fifty consecutive charge/discharge cycles. The state of the art felts showed stable performance in terms of energy efficiency and achievable capacity over the charging/discharging procedure. After 50 cycles the electrolyte was exchanged and by this measure 90% of the initial performance were recovered indicating that no significant aging of

the electrode material has occured. Unlike thermally activated carbon felts the modified neodymium oxide felts showed nearly stable charge transfer resistance and overpotentials validated by EIS measurements and polarization curves.

3.3.3. Contribution

A. Fetyan: Shared idea, experimental work, writing and discussion, and publication

3.4. Detrimental role of hydrogen evolution and its temperature-dependent impact on the performance of vanadium redox flow batteries

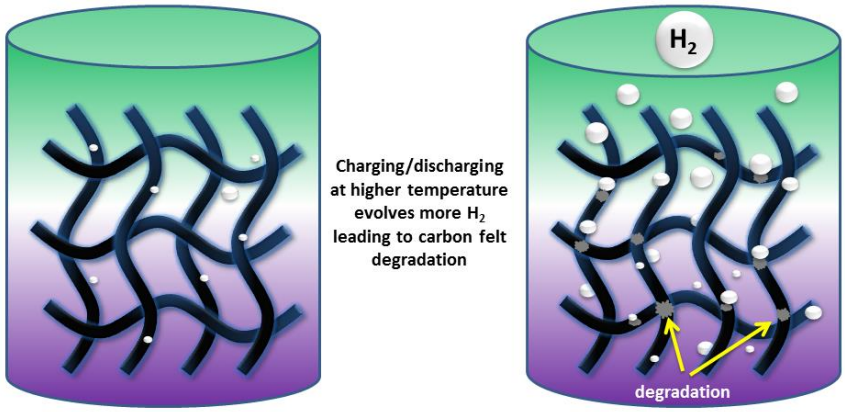

3.4.1. Motivation

Hydrogen evolution is considered the dominant parasitic side reaction and leads to different effects, such as consuming a portion of the current applied to the cell, blocking the electrode active surface area by formed gas bubbles and finally causing the imbalance of the used electrolyte. However, the effect of temperature on the rate of the side reaction and the detrimental role of this reaction on the electrode is still not reported. Understanding the role of the side reaction will help to improve the design of new electrode materials and to specify operating conditions leading to higher and more stable performance in VRFBs.

3.4.2. Description and novelties

Cyclic voltammetry measurements in a three electrode setup demonstrated that higher temperatures seem to enhance the kinetics of the vanadium redox reactions, but at the same time they significantly enhanced the rate of the undesired HER. Elevated temperatures forced the negative half-cell potential to even more negative values (-570 mV at 5 °C and ending

at -680 mV at 45 °C) indicating that the formation of hydrogen is more likely to happen. The calculated maximum achievable capacity is highest at 25 °C where a balance between many factors affected by temperature differences, such as the crossover of the vanadium ions, precipitation of V^{5+} species and HER could be achieved. The effect of evolving hydrogen on carbon felts at negative potentials for long periods of time was investigated by X-ray photoelectron spectroscopy and suggested the increase in the oxygen content, mainly (C=O). Moreover, rough surfaces were found in some regions of the carbon fibers edges as indicated by SEM images. HER was found to have a detrimental effect on the stability of the thermally activated carbon felts and hence the long-term stability of the battery.

3.4.3. Contribution

A. Fetyan: Shared idea, experimental, writing and discussion, and publication

4. Conclusion and outlook

The objective of this thesis was to find a way to increase the performance of carbon materials used as electrode for VRFBs and to understand the effect of the side reaction on the performance of the cell. The performance enhancement was achieved by two different approaches. The first approach was preparation of carbon nanofibers with high surface areas by the electrospinning technique, where cheap carbon-carbon composite fibers were synthesized based on polyacrylonitrile and carbon black powder as carbon precursors. The second approach was modifying commercial carbon felts with neodymium oxide nanoparticles by a chemical precipitation method. In the last chapter the effect of the parasitic side reaction of hydrogen evolution in the negative half-cell of the vanadium redox flow battery on the performance of the commercial carbon felt electrodes was studied at different temperatures.

As a first step, free-standing conductive ES-CNFs networks were successfully electrospun using PAN as the carbon precursor. The electrochemical activity and the performance of the produced networks were investigated by CV and charge/discharge cycles and compared to the performance of commercial CF. Three electrode cell results for the negative electrode reaction showed that the activity was much lower for CF, whereas the use of ES-CNFs showed a noticeable improvement and clear redox peaks. Higher discharge capacity and energy efficiency for the ES-CNFs compared to CF was evident by charge/discharge investigations at current density of 15 mA cm^{-2}. Scanning electron microscopy, XRD and Raman spectroscopy data demonstrated mechanical stability and electrochemical activity of the ES-CNF structure over five cycles. Exposing ES-CNFs to an acidic medium led to the removal of amorphous carbons from the samples indicating a positive long term performance of the felt. Adding a cheap carbon precursor which have significant positive effect on the activity of the fabricated material and reduce the cost of the final product was accomplished using poly acrylic acid as a binder polymer which degrades at elevated temperature during the carbonization step leaving a mixture of carbon-carbon (C-C) composite material behind.

The novel electrode was characterized by scanning electron microscopy, the fibers exhibiting rough and twisted surfaces with an average diameter in the range of 750 nm. Promising performance in the three electrode setup demonstrated its potential use as positive and negative electrode in VRFBs when compared to pristine and heat-treated commercial carbon felts. Comparable performances to the commercial CF were only obtained at current densities below 60 mA cm^{-2} in a realistic battery tester. Transport properties and simulated electrolyte

flow in both ES-CNFs and commercial carbon felt were obtained using X-ray computed tomography and open source pore network modelling. Smaller pore sizes and therefore lower electrolyte transport in ES-CNFs was concluded from the data analysis, an issue which can be correlated to the low performance of ES-CNFs at relatively high current density.

In the second approach, commercial CFs were successfully modified with neodymium-oxide to improve their electrochemical activity and stability towards both V(IV)/V(V) and V(II)/V(III) redox couples and to decrease the felt's degradation over time. The presence of well distributed Nd_2O_3 nano-particles and the lack of signs of agglomeration on the surface of the fibers were evident by SEM, EDX and XRD measurements. Three electrode setup and realistic battery test measurements showed significantly enhanced performance of Nd_2O_3-CF electrodes in terms of energy efficiency and charge/discharge capacities over 50 charge/discharge cycles. Compared to HT-CF electrodes, a lower charge transfer resistance was also observed for the Nd_2O_3-CF after 50 charge/discharge cycles. Furthermore, when the electrolyte was replaced by fresh one after 50 cycles, the Nd_2O_3-CFs could retrieve their original performance. This indicated that less degradation occurred in the Nd_2O_3-CFs modified felts and that they maintained their oxygen-donating functionalities in contrast to the thermally activated CF. This improved performance is linked to the strong binding between the neodymium and oxygen providing functional groups on the surface of the fibers, working as highly active sites for the vanadium redox reactions.

Finally the electrochemical performance of thermally activated commercial CF was studied in three electrode setup at different temperatures; cyclic voltammetry analysis showed an enhancement in the kinetics of both redox reactions of V(II)/V (III) and V(IV)/V(V) at higher temperature, simultaneously with enhanced catalytic performance of the undesired HER in the negative half-cell. In battery test measurements, the same trend with higher temperatures was demonstrated. The decreased coulombic efficiency at elevated temperatures was associated to hydrogen formation in the negative half-cell. The negative shift of maximum half-cell potentials recorded in the negative side indicates that the formation of hydrogen is more likely at higher temperature. The effect of hydrogen evolution formation on the fibers surface of thermally activated CF was studied at different temperatures, and the SEM images linked to XPS analysis illustrated the degradation of the felt’s surface, loss in conductive carbon and higher degree of oxidation on the surface of the fibers.

Electrolyte flow and penetration in the CFs is a key factor in boosting the performance of the electrode material. Increasing the pore size between the produced ES-CNFs as well as

increasing the fraction of functional surface groups which in turn enhances the wettability of the felts and its water penetration will result in improving the performance of ES-CNFs at higher current density. An issue which can be achieved in various approaches; for instance, introducing larger pore sizes to the ES-CNFs is believed to be achievable by using additional polymer which can be removed after electrospinning using specific solvent. Combining both approaches in this thesis where mixing metal or metal oxide to the polymer solution to produce doped electrospun fibers which can be then carbonized is supposed to increase the wettability of the material and present stable active sites which can play a positive role to the overall activity and performance. This could be accompanied with further investigations on the effectiveness of the introduced catalysts at different temperatures to avoid the evolution of hydrogen and to prevent the oxidation of the fibers.

5. Acknowledgments

This work is the fruit of beautiful years spent in the laboratories of “Freie Universität Berlin” where I had the chance to participate in various projects.

I would like first to warmly thank Professor Christina Roth for having me in her team. I am grateful for her trust, encouragement, and constant support during this work.

My thanks also go to the members of the committee who accepted evaluating and judging my dissertation.

I would also like to thank my colleagues for their help and support. It was great time and a very nice experience.

I also think of all my friends who accompanied me during all these years and would like to thank them for their advices and good thoughts.

My last but not least thanks are for my family who stood by me. I would not have made it without their unconditional support and encouragement; my lovely wife and my little son who inspired and empowered me and brought me the joy and happiness all the time, my father who taught me to always keep up and work hard, my mother who believed in me and always supported me to keep going and achieve my goals.

Thank you

6. Literature

1. Weber, A. Z.; Mench, M. M.; Meyers, J. P.; Ross, P. N.; Gostick, J. T.; Liu, Q., Redox flow batteries: a review. *Journal of Applied Electrochemistry* **2011,** *41* (10), 1137.
2. Derr, I., Electrochemical degradation and chemical aging of carbon felt electrodes in all-vanadium redox flow batteries. *Freie Universität Berlin* **2017,** *Doctoral dissertation*, Berlin, Germany.
3. Ponce de León, C.; Frías-Ferrer, A.; González-García, J.; Szánto, D. A.; Walsh, F. C., Redox flow cells for energy conversion. *Journal of Power Sources* **2006,** *160* (1), 716-732.
4. Alotto, P.; Guarnieri, M.; Moro, F., Redox flow batteries for the storage of renewable energy: A review. *Renewable and Sustainable Energy Reviews* **2014,** *29*, 325-335.
5. Soloveichik, G. L., Flow Batteries: Current Status and Trends. *Chemical Reviews* **2015,** *115* (20), 11533-11558.
6. Kear, G.; Shah, A. A.; Walsh, F. C., Development of the all-vanadium redox flow battery for energy storage: a review of technological, financial and policy aspects. *International Journal of Energy Research* **2012,** *36* (11), 1105-1120.
7. Noack, J.; Roznyatovskaya, N.; Herr, T.; Fischer, P., The Chemistry of Redox-Flow Batteries. *Angewandte Chemie International Edition* **2015,** *54* (34), 9776-9809.
8. Sun, B.; Skyllas-Kazacos, M., Chemical modification of graphite electrode materials for vanadium redox flow battery application—part II. Acid treatments. *Electrochimica Acta* **1992,** *37* (13), 2459-2465.
9. Di Blasi, A.; Di Blasi, O.; Briguglio, N.; Aricò, A. S.; Sebastián, D.; Lázaro, M. J.; Monforte, G.; Antonucci, V., Investigation of several graphite-based electrodes for vanadium redox flow cell. *Journal of Power Sources* **2013,** *227*, 15-23.
10. Sun, B.; Skyllas-Kazacos, M., Modification of graphite electrode materials for vanadium redox flow battery application—I. Thermal treatment. *Electrochimica Acta* **1992,** *37* (7), 1253-1260.
11. Sun, B.; Skyllas-Kazakos, M., Chemical modification and electrochemical behaviour of graphite fibre in acidic vanadium solution. *Electrochimica Acta* **1991,** *36* (3), 513-517.
12. Wang, W. H.; Wang, X. D., Investigation of Ir-modified carbon felt as the positive electrode of an all-vanadium redox flow battery. *Electrochimica Acta* **2007,** *52* (24), 6755-6762.
13. Zhou, H.; Shen, Y.; Xi, J.; Qiu, X.; Chen, L., ZrO2-Nanoparticle-Modified Graphite Felt: Bifunctional Effects on Vanadium Flow Batteries. *ACS Applied Materials & Interfaces* **2016,** *8* (24), 15369-15378.
14. Li, B.; Gu, M.; Nie, Z.; Wei, X.; Wang, C.; Sprenkle, V.; Wang, W., Nanorod Niobium Oxide as Powerful Catalysts for an All Vanadium Redox Flow Battery. *Nano Letters* **2014,** *14* (1), 158-165.
15. Zhang, W.; Xi, J.; Li, Z.; Zhou, H.; Liu, L.; Wu, Z.; Qiu, X., Electrochemical activation of graphite felt electrode for VO2+/VO2+ redox couple application. *Electrochimica Acta* **2013,** *89*, 429-435.
16. Derr, I.; Przyrembel, D.; Schweer, J.; Fetyan, A.; Langner, J.; Melke, J.; Weinelt, M.; Roth, C., Electroless chemical aging of carbon felt electrodes for the all-vanadium redox flow battery (VRFB) investigated by Electrochemical Impedance and X-ray Photoelectron Spectroscopy. *Electrochimica Acta* **2017,** *246*, 783-793.
17. Derr, I.; Bruns, M.; Langner, J.; Fetyan, A.; Melke, J.; Roth, C., Degradation of all-vanadium redox flow batteries (VRFB) investigated by electrochemical impedance and X-ray photoelectron spectroscopy: Part 2 electrochemical degradation. *Journal of Power Sources* **2016,** *325*, 351-359.
18. Taylor, S. M.; Pătru, A.; Fabbri, E.; Schmidt, T. J., Influence of surface oxygen groups on V(II) oxidation reaction kinetics. *Electrochemistry Communications* **2017,** *75*, 13-16.

19. Skyllas-Kazacos, M.; Chakrabarti, M. H.; Hajimolana, S. A.; Mjalli, F. S.; Saleem, M., Progress in Flow Battery Research and Development. *Journal of The Electrochemical Society* **2011,** *158* (8), R55-R79.
20. Leung, P.; Li, X.; Ponce de León, C.; Berlouis, L.; Low, C. T. J.; Walsh, F. C., Progress in redox flow batteries, remaining challenges and their applications in energy storage. *RSC Advances* **2012,** *2* (27), 10125-10156.
21. Wang, W.; Luo, Q.; Li, B.; Wei, X.; Li, L.; Yang, Z., Recent Progress in Redox Flow Battery Research and Development. *Advanced Functional Materials* **2013,** *23* (8), 970-986.
22. Soloveichik, G. L., Battery Technologies for Large-Scale Stationary Energy Storage. *Annual Review of Chemical and Biomolecular Engineering* **2011,** *2* (1), 503-527.
23. Ding, C.; Zhang, H.; Li, X.; Liu, T.; Xing, F., Vanadium Flow Battery for Energy Storage: Prospects and Challenges. *The Journal of Physical Chemistry Letters* **2013,** *4* (8), 1281-1294.
24. Skyllas-Kazacos, M.; Menictas, C.; Kazacos, M., Thermal Stability of Concentrated V(V) Electrolytes in the Vanadium Redox Cell. *Journal of The Electrochemical Society* **1996,** *143* (4), L86-L88.
25. Skyllas-Kazacos, M.; Peng, C.; Cheng, M., Evaluation of Precipitation Inhibitors for Supersaturated Vanadyl Electrolytes for the Vanadium Redox Battery. *Electrochemical and Solid-State Letters* **1999,** *2* (3), 121-122.
26. Vijayakumar, M.; Wang, W.; Nie, Z.; Sprenkle, V.; Hu, J., Elucidating the higher stability of vanadium(V) cations in mixed acid based redox flow battery electrolytes. *Journal of Power Sources* **2013,** *241*, 173-177.
27. Li, L.; Kim, S.; Wang, W.; Vijayakumar, M.; Nie, Z.; Chen, B.; Zhang, J.; Xia, G.; Hu, J.; Graff, G.; Liu, J.; Yang, Z., A Stable Vanadium Redox-Flow Battery with High Energy Density for Large-Scale Energy Storage. *Advanced Energy Materials* **2011,** *1* (3), 394-400.
28. Park, S.-K.; Shim, J.; Yang, J. H.; Jin, C.-S.; Lee, B. S.; Lee, Y.-S.; Shin, K.-H.; Jeon, J.-D., The influence of compressed carbon felt electrodes on the performance of a vanadium redox flow battery. *Electrochimica Acta* **2014,** *116*, 447-452.
29. Chang, T.-C.; Zhang, J.-P.; Fuh, Y.-K., Electrical, mechanical and morphological properties of compressed carbon felt electrodes in vanadium redox flow battery. *Journal of Power Sources* **2014,** *245*, 66-75.
30. Tang, A.; Bao, J.; Skyllas-Kazacos, M., Studies on pressure losses and flow rate optimization in vanadium redox flow battery. *Journal of Power Sources* **2014,** *248*, 154-162.
31. Zhang, J.; Zhou, T.; Xia, L.; Yuan, C.; Zhang, W.; Zhang, A., Polypropylene elastomer composite for the all-vanadium redox flow battery: current collector materials. *Journal of Materials Chemistry A* **2015,** *3* (5), 2387-2398.
32. Satola, B.; Komsiyska, L.; Wittstock, G., Corrosion of Graphite-Polypropylene Current Collectors during Overcharging in Negative and Positive Vanadium Redox Flow Battery Half-Cell Electrolytes. *Journal of The Electrochemical Society* **2018,** *165* (5), A963-A969.
33. Ulaganathan, M.; Aravindan, V.; Yan, Q.; Madhavi, S.; Skyllas-Kazacos, M.; Lim, T. M., Recent Advancements in All-Vanadium Redox Flow Batteries. *Advanced Materials Interfaces* **2016,** *3* (1), 1500309.
34. Lee, N. J. L., Seung-Wook; Kim, Ki Jae; Kim, Jae-Hun; Park, Min-Sik; Jeong, Goojin; Kim, Young-Jun; Byun, Dongjin;, Development of Carbon Composite Bipolar Plates for Vanadium Redox Flow Batteries. *Bulletin of the Korean Chemical Society* **2012,** *33* (11), 3589-3592.
35. Rudolph, S.; Schröder, U.; Bayanov, I. M.; Pfeiffer, G., Corrosion prevention of graphite collector in vanadium redox flow battery. *Journal of Electroanalytical Chemistry* **2013,** *709*, 93-98.

36. Nam, S.; Lee, D.; Lee, D. G.; Kim, J., Nano carbon/fluoroelastomer composite bipolar plate for a vanadium redox flow battery (VRFB). *Composite Structures* **2017,** *159*, 220-227.
37. Lim, J. W.; Lee, D. G., Carbon fiber/polyethylene bipolar plate-carbon felt electrode assembly for vanadium redox flow batteries (VRFB). *Composite Structures* **2015,** *134*, 483-492.
38. Lee, D.; Lee, D. G.; Lim, J. W., Development of multifunctional carbon composite bipolar plate for vanadium redox flow batteries. *Journal of Intelligent Material Systems and Structures 0* (0), 1045389X17708345.
39. Haddadi-Asl, V.; Kazacos, M.; Skyllas-Kazacos, M., Carbon–polymer composite electrodes for redox cells. *Journal of Applied Polymer Science* **1995,** *57* (12), 1455-1463.
40. Chakrabarti, M. H.; Brandon, N. P.; Hajimolana, S. A.; Tariq, F.; Yufit, V.; Hashim, M. A.; Hussain, M. A.; Low, C. T. J.; Aravind, P. V., Application of carbon materials in redox flow batteries. *Journal of Power Sources* **2014,** *253*, 150-166.
41. Sukkar, T.; Skyllas-Kazacos, M., Water transfer behaviour across cation exchange membranes in the vanadium redox battery. *Journal of Membrane Science* **2003,** *222* (1), 235-247.
42. Xi, J.; Wu, Z.; Teng, X.; Zhao, Y.; Chen, L.; Qiu, X., Self-assembled polyelectrolyte multilayer modified Nafion membrane with suppressed vanadium ion crossover for vanadium redox flow batteries. *Journal of Materials Chemistry* **2008,** *18* (11), 1232-1238.
43. Sukkar, T.; Skyllas-Kazacos, M., Membrane stability studies for vanadium redox cell applications. *Journal of Applied Electrochemistry* **2004,** *34* (2), 137-145.
44. Ngamsai, K.; Arpornwichanop, A., Analysis and measurement of the electrolyte imbalance in a vanadium redox flow battery. *Journal of Power Sources* **2015,** *282*, 534-543.
45. Roznyatovskaya, N.; Herr, T.; Küttinger, M.; Fühl, M.; Noack, J.; Pinkwart, K.; Tübke, J., Detection of capacity imbalance in vanadium electrolyte and its electrochemical regeneration for all-vanadium redox-flow batteries. *Journal of Power Sources* **2016,** *302*, 79-83.
46. Sun, C.; Chen, J.; Zhang, H.; Han, X.; Luo, Q., Investigations on transfer of water and vanadium ions across Nafion membrane in an operating vanadium redox flow battery. *Journal of Power Sources* **2010,** *195* (3), 890-897.
47. Tian, B.; Yan, C. W.; Wang, F. H., Proton conducting composite membrane from Daramic/Nafion for vanadium redox flow battery. *Journal of Membrane Science* **2004,** *234* (1), 51-54.
48. Xi, J.; Wu, Z.; Qiu, X.; Chen, L., Nafion/SiO2 hybrid membrane for vanadium redox flow battery. *Journal of Power Sources* **2007,** *166* (2), 531-536.
49. Seo, S.-J.; Kim, B.-C.; Sung, K.-W.; Shim, J.; Jeon, J.-D.; Shin, K.-H.; Shin, S.-H.; Yun, S.-H.; Lee, J.-Y.; Moon, S.-H., Electrochemical properties of pore-filled anion exchange membranes and their ionic transport phenomena for vanadium redox flow battery applications. *Journal of Membrane Science* **2013,** *428*, 17-23.
50. Sukkar, T.; Skyllas-Kazacos, M., Modification of membranes using polyelectrolytes to improve water transfer properties in the vanadium redox battery. *Journal of Membrane Science* **2003,** *222* (1), 249-264.
51. Chieng, S. C.; Kazacos, M.; Skyllas-Kazacos, M., Preparation and evaluation of composite membrane for vanadium redox battery applications. *Journal of Power Sources* **1992,** *39* (1), 11-19.
52. Chieng, S. C.; Kazacos, M.; Skyllas-Kazacos, M., Modification of Daramic, microporous separator, for redox flow battery applications. *Journal of Membrane Science* **1992,** *75* (1), 81-91.
53. Mohammadi, T.; Skyllas-Kazacos, M., Preparation of sulfonated composite membrane for vanadium redox flow battery applications. *Journal of Membrane Science* **1995,** *107* (1), 35-45.

54. Kim, K. J.; Park, M.-S.; Kim, Y.-J.; Kim, J. H.; Dou, S. X.; Skyllas-Kazacos, M., A technology review of electrodes and reaction mechanisms in vanadium redox flow batteries. *Journal of Materials Chemistry A* **2015,** *3* (33), 16913-16933.
55. Zhu, H. Q.; Zhang, Y. M.; Yue, L.; Li, W. S.; Li, G. L.; Shu, D.; Chen, H. Y., Graphite–carbon nanotube composite electrodes for all vanadium redox flow battery. *Journal of Power Sources* **2008,** *184* (2), 637-640.
56. Flox, C.; Skoumal, M.; Rubio-Garcia, J.; Andreu, T.; Morante, J. R., Strategies for enhancing electrochemical activity of carbon-based electrodes for all-vanadium redox flow batteries. *Applied Energy* **2013,** *109*, 344-351.
57. Lv, Y.; Zhang, J.; Lv, Z.; Wu, C.; Liu, Y.; Wang, H.; Lu, S.; Xiang, Y., Enhanced electrochemical activity of carbon felt for V2+/V3+ redox reaction via combining KOH-etched pretreatment with uniform deposition of Bi nanoparticles. *Electrochimica Acta* **2017,** *253*, 78-84.
58. Shen, J.; Liu, S.; He, Z.; Shi, L., Influence of antimony ions in negative electrolyte on the electrochemical performance of vanadium redox flow batteries. *Electrochimica Acta* **2015,** *151*, 297-305.
59. Flox, C.; Rubio-Garcia, J.; Nafria, R.; Zamani, R.; Skoumal, M.; Andreu, T.; Arbiol, J.; Cabot, A.; Morante, J. R., Active nano-CuPt3 electrocatalyst supported on graphene for enhancing reactions at the cathode in all-vanadium redox flow batteries. *Carbon* **2012,** *50* (6), 2372-2374.
60. Shen, Y.; Xu, H.; Xu, P.; Wu, X.; Dong, Y.; Lu, L., Electrochemical catalytic activity of tungsten trioxide- modified graphite felt toward VO2+/VO2+ redox reaction. *Electrochimica Acta* **2014,** *132*, 37-41.
61. Lee, W.; Jo, C.; Youk, S.; Shin, H. Y.; Lee, J.; Chung, Y.; Kwon, Y., Mesoporous tungsten oxynitride as electrocatalyst for promoting redox reactions of vanadium redox couple and performance of vanadium redox flow battery. *Applied Surface Science* **2018,** *429*, 187-195.
62. Kim, K. J.; Park, M.-S.; Kim, J.-H.; Hwang, U.; Lee, N. J.; Jeong, G.; Kim, Y.-J., Novel catalytic effects of Mn3O4 for all vanadium redox flow batteries. *Chemical Communications* **2012,** *48* (44), 5455-5457.
63. Di Blasi, A.; Briguglio, N.; Di Blasi, O.; Antonucci, V., Charge–discharge performance of carbon fiber-based electrodes in single cell and short stack for vanadium redox flow battery. *Applied Energy* **2014,** *125*, 114-122.
64. Fuyu Chen, J. L., Hui Chen, Chuanwei Yan, Study on Hydrogen Evolution Reaction at a Graphite Electrode in the All-Vanadium Redox Flow Battery. *International Journal of Electrochemical Science* **2012,** *7*, 3750 - 3764.
65. Schweiss, R.; Pritzl, A.; Meiser, C., Parasitic Hydrogen Evolution at Different Carbon Fiber Electrodes in Vanadium Redox Flow Batteries. *Journal of The Electrochemical Society* **2016,** *163* (9), A2089-A2094.
66. Sun, C.-N.; Delnick, F. M.; Baggetto, L.; Veith, G. M.; Zawodzinski, T. A., Hydrogen evolution at the negative electrode of the all-vanadium redox flow batteries. *Journal of Power Sources* **2014,** *248*, 560-564.
67. Gattrell, M.; Park, J.; MacDougall, B.; Apte, J.; McCarthy, S.; Wu, C. W., Study of the Mechanism of the Vanadium 4+/5+ Redox Reaction in Acidic Solutions. *Journal of The Electrochemical Society* **2004,** *151* (1), A123-A130.
68. Langner, J., Kohlenstoffbasierte Faser-Elektroden für Vanadium Redoxflow Batterien. *Karlsruher Institut für Technologie* **2016,** *Doctoral dissertation*, Karlsruhe, Germany.
69. Blanc, C., Modeling of a Vanadium Redox Flow Battery Electricity Storage System. *ÉCOLE POLYTECHNIQUE FÉDÉRALE DE LAUSANNE* **2009,** *Doctoral dissertation*, Lausanne, Switzerland.

70. Gattrell, M.; Qian, J.; Stewart, C.; Graham, P.; MacDougall, B., The electrochemical reduction of VO2+ in acidic solution at high overpotentials. *Electrochimica Acta* **2005,** *51* (3), 395-407.
71. McCreery, R. L., Advanced Carbon Electrode Materials for Molecular Electrochemistry. *Chemical Reviews* **2008,** *108* (7), 2646-2687.
72. Beguin, F.; Frackowiak, E., *Carbons for Electrochemical Energy Storage and Conversion Systems*. CRC press,Taylor & Francis Group: United States of America, **2009**.
73. Gorss, J., High Performance Carbon Fibers. *American Chemical Society* **2003**.
74. Karacan, I.; Erdogan, G., The influence of thermal stabilization stage on the molecular structure of polyacrylonitrile fibers prior to the carbonization stage. *Fibers and Polymers* **2012,** *13* (3), 295-302.
75. Jain, M. K.; Balasubramanian, M.; Desai, P.; Abhiraman, A. S., Conversion of acrylonitrile-based precursors to carbon fibres. *Journal of Materials Science* **1987,** *22* (1), 301-312.
76. Rahaman, M. S. A.; Ismail, A. F.; Mustafa, A., A review of heat treatment on polyacrylonitrile fiber. *Polymer Degradation and Stability* **2007,** *92* (8), 1421-1432.
77. Li, D.; Xia, Y., Electrospinning of Nanofibers: Reinventing the Wheel? *Advanced Materials* **2004,** *16* (14), 1151-1170.
78. P. Heikkilä, A. H., Electrospinning of polyacrylonitrile (PAN) solution: Effect of conductive additive and filler on the process. *eXPRESS Polymer Letters* **2009,** *3* (7), 437–445.
79. Huang, Z.-M.; Zhang, Y. Z.; Kotaki, M.; Ramakrishna, S., A review on polymer nanofibers by electrospinning and their applications in nanocomposites. *Composites Science and Technology* **2003,** *63* (15), 2223-2253.
80. Darrell, H. R.; Iksoo, C., Nanometre diameter fibres of polymer, produced by electrospinning. *Nanotechnology* **1996,** *7* (3), 216.
81. Frenot, A.; Chronakis, I. S., Polymer nanofibers assembled by electrospinning. *Current Opinion in Colloid & Interface Science* **2003,** *8* (1), 64-75.
82. Doshi, J.; Reneker, D. H., Electrospinning process and applications of electrospun fibers. *Journal of Electrostatics* **1995,** *35* (2), 151-160.
83. Dosunmu, O. O.; Chase, G. G.; Kataphinan, W.; Reneker, D. H., Electrospinning of polymer nanofibres from multiple jets on a porous tubular surface. *Nanotechnology* **2006,** *17* (4), 1123.
84. Nurwaha, D.; Han, W.; Wang, X., Investigation of a New Needleless Electrospinning Method for the Production of Nanofibers. *Journal of Engineered Fibers and Fabrics* **2013,** *8* (4), 42-49.
85. Liu, H.; Mukherjee, S.; Liu, Y.; Ramakrishna, S., Recent studies on electrospinning preparation of patterned, core–shell, and aligned scaffolds. *Journal of Applied Polymer Science* **2018,** *135* (31), 46570.
86. Kim, J.-S.; Reneker, D. H., Polybenzimidazole nanofiber produced by electrospinning. *Polymer Engineering & Science* **1999,** *39* (5), 849-854.
87. Li, D.; Wang, Y.; Xia, Y., Electrospinning of Polymeric and Ceramic Nanofibers as Uniaxially Aligned Arrays. *Nano Letters* **2003,** *3* (8), 1167-1171.
88. Li, D.; Wang, Y.; Xia, Y., Electrospinning Nanofibers as Uniaxially Aligned Arrays and Layer-by-Layer Stacked Films. *Advanced Materials* **2004,** *16* (4), 361-366.
89. Singhal, R.; Kalra, V., Cobalt Nanoparticles Embedded in Porous Carbon Nanofibers As Bifunctional Electrocatalysts for Oxygen Reduction and Evolution Reactions. *Meeting Abstracts* **2015,** *MA2015-02* (1), 28.
90. Ju, Y.-W.; Yoo, S.; Kim, C.; Kim, S.; Jeon, I.-Y.; Shin, J.; Baek, J.-B.; Kim, G., Fe@N-Graphene Nanoplatelet-Embedded Carbon Nanofibers as Efficient Electrocatalysts for Oxygen Reduction Reaction. *Advanced Science* **2016,** *3* (1), 1500205.

91. Zhao, Y.; Lai, Q.; Wang, Y.; Zhu, J.; Liang, Y., Interconnected Hierarchically Porous Fe, N-Codoped Carbon Nanofibers as Efficient Oxygen Reduction Catalysts for Zn–Air Batteries. *ACS Applied Materials & Interfaces* **2017,** *9* (19), 16178-16186.
92. Li, D.; McCann, J. T.; Gratt, M.; Xia, Y., Photocatalytic deposition of gold nanoparticles on electrospun nanofibers of titania. *Chemical Physics Letters* **2004,** *394* (4), 387-391.
93. Self, E. C.; Wycisk, R.; Pintauro, P. N., Electrospun titania-based fibers for high areal capacity Li-ion battery anodes. *Journal of Power Sources* **2015,** *282*, 187-193.
94. Wei, G.; Fan, X.; Liu, J.; Yan, C., Electrospun carbon nanofibers/electrocatalyst hybrids as asymmetric electrodes for vanadium redox flow battery. *Journal of Power Sources* **2015,** *281*, 1-6.
95. Sun, Z.; Zussman, E.; Yarin, A. L.; Wendorff, J. H.; Greiner, A., Compound Core–Shell Polymer Nanofibers by Co-Electrospinning. *Advanced Materials* **2003,** *15* (22), 1929-1932.
96. Li, D.; Xia, Y., Direct Fabrication of Composite and Ceramic Hollow Nanofibers by Electrospinning. *Nano Letters* **2004,** *4* (5), 933-938.
97. Hou, H.; Jun, Z.; Reuning, A.; Schaper, A.; Wendorff, J. H.; Greiner, A., Poly(p-xylylene) Nanotubes by Coating and Removal of Ultrathin Polymer Template Fibers. *Macromolecules* **2002,** *35* (7), 2429-2431.
98. Caruso, R. A.; Schattka, J. H.; Greiner, A., Titanium Dioxide Tubes from Sol–Gel Coating of Electrospun Polymer Fibers. *Advanced Materials* **2001,** *13* (20), 1577-1579.
99. Dong, H.; Prasad, S.; Nyame, V.; Jones, W. E., Sub-micrometer Conducting Polyaniline Tubes Prepared from Polymer Fiber Templates. *Chemistry of Materials* **2004,** *16* (3), 371-373.
100. Wang, J., *Analytical Electrochemistry*. 2nd edition ed.; Wiley-VCH 2001: New York **2001**.
101. Elgrishi, N.; Rountree, K. J.; McCarthy, B. D.; Rountree, E. S.; Eisenhart, T. T.; Dempsey, J. L., A Practical Beginner's Guide to Cyclic Voltammetry. *Journal of Chemical Education* **2018,** *95* (2), 197-206.
102. Friedl, J.; Stimming, U., Determining Electron Transfer Kinetics at Porous Electrodes. *Electrochimica Acta* **2017,** *227*, 235-245.
103. Smith, E.; Dent, G., *Modern Raman Spectroscopy - A Practical Approach*. John Wiley & Sons, Ltd West Sussex, England, **2005**.
104. Sadezky, A.; Muckenhuber, H.; Grothe, H.; Niessner, R.; Pöschl, U., Raman microspectroscopy of soot and related carbonaceous materials: Spectral analysis and structural information. *Carbon* **2005,** *43* (8), 1731-1742.
105. Vernon-Parry, K. D., Scanning electron microscopy: an introduction. *Centre for Electronic Materials, UMIST* **2000,** *13* (4), 40-44.
106. Egerton, R. F., *Physical principles of electron microscopy : an introduction to TEM, SEM, and AEM*. Springer: US, **2005**.
107. Reimer, L., *Scanning electron microscopy : physics of image formation and microanalysis*. Springer: Berlin Heidelberg, **1998**.
108. du Plessis, A.; Broeckhoven, C.; Guelpa, A.; le Roux, S. G., Laboratory x-ray micro-computed tomography: a user guideline for biological samples. *GigaScience* **2017,** *6* (6), 1-11.
109. Landis, E. N.; Keane, D. T., X-ray microtomography. *Materials Characterization* **2010,** *61* (12), 1305-1316.

Included publications reprints

Electrospun carbon nanofibers as alternative electrode materials for vanadium redox flow batteries

Abstract

Non-woven carbon nanofiber networks were produced by electrospinning. Electrospinning is a process that can easily be up-scaled, producing carbon fibers that can be used as electrodes with increased surface area and reaction sites. The structure of electrospun carbon nanofibers (ES-CNFs) was investigated by scanning electron microscopy and compared to a commercial carbon felt (CF). The electrochemical properties of the obtained ES-CNFs were studied for the negative half-cell reaction in a three-electrode setup and a single-cell battery test system. The performance and stability of the generated materials were tested by charging and discharging the cell and carrying out X-ray diffraction and Raman spectroscopy before and after operation. An increase in the energy efficiency of about 10% was achieved when using five sheets of free-standing ES-CNFs compared to commercial CFs, revealing the potential use of ES-CNFs as electrode materials in the negative half-cell of all-vanadium redox flow batteries.

Reference:

Fetyan, A.; Derr, I.; Kayarkatte, M. K.; Langner, J.; Bernsmeier, D.; Kraehnert, R.; Roth, C., Electrospun Carbon Nanofibers as Alternative Electrode Materials for Vanadium Redox Flow Batteries. ChemElectroChem 2015, 2 (12), 2055-2060.

https://doi.org/10.1002/celc.201500284

Comparison of Electrospun Carbon−Carbon Composite and Commercial Felt for Their Activity and Electrolyte Utilization in Vanadium Redox Flow Batteries

Abstract

A low cost highly active carbon-carbon composite fiber felt was produced by electrospinning a mixture of polyacrylonitrile and carbon black powder using poly acrylic acid as a binder for high carbon black loading. The newly designed high-surface area electrode material showed promising results for use as electrode material for both the negative and positive half-cell of vanadium redox flow batteries. Battery test results demonstrated promising performance for the electrospun carbon fibers at current densities below 60 $mAcm^{-2}$, but were less active at higher values. The microstructure of the felt was characterized by X-ray computed tomography to obtain the porous pathways, which facilitate electrolyte transport. The obtained results will help us to understand the role of porosity in the performance of the battery and to consequently improve the design of the carbon-filled electrospun material.

Reference:

Fetyan, A.; Schneider, J.; Schnucklake, M.; El-Nagar, G. A.; Banerjee, R.; Bevilacqua, N.; Zeis, R.; Roth, C., Comparison of Electrospun Carbon−Carbon Composite and Commercial Felt for Their Activity and Electrolyte Utilization in Vanadium Redox Flow Batteries. ChemElectroChem 2019, 6, 130-135.

https://doi.org/10.1002/celc.201801128

A neodymium oxide nanoparticle-doped carbon felt as promising electrode for vanadium redox flow batteries

Abstract

Neodymium oxide (Nd_2O_3) nanoparticles were chemically embedded on a state-of-the art carbon felt (CF) by a precipitation method in non-aqueous solution. Different Nd_2O_3 loadings were chosen and the obtained electrocatalyst-loaded felts tested for application as electrode in all-vanadium redox flow batteries. Cyclic voltammetry (CV) studies confirmed that Nd_2O_3 has a catalytic effect towards both redox couples, V^{4+}/V^{5+} at the positive and V^{2+}/V^{3+} at the negative side. Scanning electron microscopy (SEM), energy dispersive X-ray spectroscopy (EDX) and X-ray diffraction (XRD) demonstrated only minor particle agglomeration and high dispersion of the particles on the fibres. Charge/discharge profiles revealed an enhanced performance with higher discharge capacity and higher energy efficiency for the modified felts when compared to a thermally activated CF. For instance, after 50 consecutive charge/discharge cycles the energy efficiency of the Nd_2O_3 modified carbon felt (Nd_2O_3-CF) was reduced only by 3% compared to a 12% irreversible loss observed for the thermally activated CF. After exchanging the electrolyte after 50 cycles, the felts retained their original performance indicating that less degradation occurred in the modified felts than in the industrial standard and that they maintained their oxygen-donating functionalities on the surface as compared to thermally activated CF.

Reference:

Fetyan, A.; El-Nagar, G. A.; Derr, I.; Kubella, P.; Dau, H.; Roth, C., A neodymium oxide nanoparticle-doped carbon felt as promising electrode for vanadium redox flow batteries. Electrochimica Acta 2018, 268, 59-65.

https://doi.org/10.1016/j.electacta.2018.02.104

Detrimental role of hydrogen evolution and its temperature-dependent impact on the performance of vanadium redox flow batteries

Abstract

This paper addresses the damaging role of the parasitic hydrogen evolution reaction (HER) in the negative half-cell of a vanadium redox flow battery (VRFB) on state-of-the-art carbon felt electrodes at different temperatures. It was found that increasing the temperature resulted in a better catalytic performance for both the positive and negative half-cell reactions. In addition, increasing the temperature significantly enhanced the undesired HER at the negative side. Operating the VRFB cell at higher temperature led to a decrease in the coulombic efficiency attributed to the higher hydrogen production. More pronounced hydrogen production caused an oxidation on the surface of the carbon fibers and a degradation of the electrode as indicated from scanning electron microscopy and X-ray photoelectron spectroscopy measurements. This observed degradation results in fading of the overall performance of the vanadium redox flow battery over time.

Reference:

Fetyan, A.; El-Nagar, G. A.; Lauermann, I.; Schnucklake, M.; Schneider, J.; Roth, C., Detrimental role of hydrogen evolution and its temperature-dependent impact on the performance of vanadium redox flow batteries. Journal of Energy Chemistry 2018 (accepted).

https://doi.org/10.1016/j.jechem.2018.06.010